Mechanistic insights into light-driven allosteric control of GPCR biological activity

Maria Ricart-Ortega, Alice Berizzi, Vanessa Pereira, Fanny Malhaire, Juanlo Catena, Joan Font, Xavier Gómez-Santacana, Lourdes Muñoz, Charleine Zussy, Carmen Serra, et al.

ACS Pharmacology and Translational Science

https://dx.doi.org/10.1021/acsptsci.0c00054

Mechanistic insights into light-driven allosteric control of GPCR biological activity

Maria Ricart-Ortega[a,c,1], Alice E. Berizzi[c,1], Vanessa Pereira[c], Fanny Malhaire[c], Juanlo Catena[a], Joan Font[c], Xavier Gómez-Santacana[c], Lourdes Muñoz[a,b], Charleine Zussy[c], Carmen Serra[a,b], Xavier Rovira[a], Cyril Goudet[c,*] and Amadeu Llebaria[a,b,*]

[a]MCS, Laboratory of Medicinal Chemistry & Synthesis, Department of Biological Chemistry, Institute for Advanced Chemistry of Catalonia (IQAC-CSIC), Barcelona, Spain; [b]SIMchem, Service of Synthesis of High Added Value Molecules, Institute for Advanced Chemistry of Catalonia (IQAC-CSIC), Barcelona, Spain; [c]IGF, University of Montpellier, CNRS, INSERM, F-34094 Montpellier, France.

[1] equally contributed to this work

* Amadeu Llebaria (ORCID: 0000-0002-8200-4827) and Cyril Goudet (ORCID: 0000-0002-8255-3535)

Email: amadeu.llebaria@iqac.csic.es and cyril.goudet@igf.cnrs.fr

Keywords

Photopharmacology, GPCR, allostery, metabotropic glutamate receptors

Abstract

G Protein-Coupled Receptors (GPCR), including the metabotrobic glutamate 5 ($mGlu_5$) are important therapeutic targets and the development of allosteric ligands for targeting GPCRs has become a desirable approach towards modulating receptor activity. Traditional pharmacological approaches towards modulating GPCR activity are still limited since precise spatiotemporal control of a ligand is lost as soon as it is administered. Photopharmacology proposes the use of photoswitchable ligands to overcome this limitation, since their activity can be reversibly controlled by light with high precision. As this is still a growing field, our understanding of the molecular mechanisms underlying the light-induced changes in different photoswitchable ligand pharmacology is suboptimal. For this reason, we have studied the mechanisms of action of alloswitch-1 and MCS0331 two freely-diffusible, $mGlu_5$ phenylazopyridine photoswitchable negative allosteric modulators. We combined photochemical, cell-based and *in vivo* photopharmacological approaches to investigate the effects of *trans*-*cis* azobenzene photoisomerization on the functional activity and binding ability of these ligands to the $mGlu_5$ allosteric pocket. From these results, we conclude that photoisomerization can take place inside and outside the ligand binding pocket and this leads to a reversible loss in affinity, in part, due to changes in dissociation rates from the receptor. Ligand activity deviates from high-affinity $mGlu_5$ negative allosteric modulation (in the *trans*-configuration) to reduced affinity for the $mGlu_5$ in the *cis*-configuration for both photoswitchable ligands. Importantly, this mechanism translates to dynamic and reversible control over pain following local injection and illumination of negative allosteric modulators into a brain region implicated in pain control.

G Protein-Coupled Receptors (GPCR) are crucial players in cell communication and have been identified as key targets for drug discovery, with more than one third of currently available therapeutic drugs targeting them.[1] One exemplar class C GPCR is the metabotropic glutamate 5 receptor ($mGlu_5$), whose ubiquitous expression and role in regulating neuronal synaptic activity have popularised this receptor as a therapeutic target for a number of diseases that affect the central nervous system (CNS).[2-5]

The development of small molecules acting on allosteric sites on GPCRs has emerged as an attractive strategy towards modulating receptor activity. Through targeting a topographically distinct and non-overlapping binding site from that of orthosteric ligands, allosteric ligands have the potential to increase selectivity for a receptor, whilst also being capable of modulating the affinity and/or efficacy of a co-binding endogenous orthosteric ligand. For allosteric modulators without intrinsic efficacy, there is a reduced risk of receptor over-sensitization and there is an opportunity for fine-tuning endogenous signaling in a more spatiotemporal manner, which is a favorable therapeutic strategy for complex CNS disorders. [6, 7]

To date, $mGlu_5$ allosteric modulators have shown efficacy in a number of preclinical models representative of aspects of the symptomology of CNS disorders. For example, $mGlu_5$ negative allosteric modulators (NAMs) show improvements in mouse models of acute and neuropathic inflammatory pain.[4, 8] There is concern though, for potential on-target adverse effects, particularly in non-targeted tissues, relating to the use of $mGlu_5$ NAMs; their administration can impair cognition and induce psychotomimetic effects.[9, 10] This raises an important limitation to classical pharmacological approaches (i.e. small molecule ligands), where as soon as a compound is systemically administered to an organism, precise control of the activity of the ligand at its site of action or in undesired tissues is lost. Photopharmacology is emerging as an interesting approach for achieving better spatiotemporal control over drug actions for their targets.[11] It involves using ligands whose activity can be controlled by light. During illumination, the ligand may absorb a photon to trigger a photochemical reaction inducing a structural rearrangement, which can change the determinants of the molecular interaction with their receptor and hence, its biological activity. Different strategies have emerged to make a ligand photocontrollable. The more common methods involve either chemically attaching the ligand to a photocleavable cage that prevents the ligand's activity (i.e. photocaged compounds) or the incorporation of a photochromic element (typically an azobenzene moiety) into the molecular scaffold of the ligand (i.e. freely-diffusible photoswitchable or photochromic ligands) or into a linker covalently tethering the ligand to its receptor (i.e. photo-tethered compounds).[12-18]

When appropriately illuminated, freely-diffusible photoswitchable ligands can absorb photons to generate a configurational and reversible change in their structure; alternating between two isomeric forms with different shapes and molecular properties that can have opposing or different pharmacological effects at their target receptor. These ligands offer the opportunity to modulate and understand GPCR signaling in a more precise manner than classical pharmacological approaches[19, 20] since it is possible to externally operate their interaction

with the receptor. The use of light to cause photoisomerization of photochromic molecules can allow for dynamic regulation of receptor activity in a more spatiotemporal manner.[14, 21-23] Photoswitchable ligands have been developed for various GPCRs[16, 24-28], and notably for metabotropic glutamate receptors.[12, 13, 22] For example, alloswitch-1, the first molecule to be designed as a photoswitchable allosteric modulator, acts as a potent NAM of $mGlu_5$ signalling under dark conditions, in vitro, while under ultraviolet (UV) light it has reduced NAM activity.[7a, 7b] This reversible NAM activity is believed to underlie alloswitch-1's ability to reversibly modulate the behaviour of freely moving Xenopus tropicalis tadpoles, zebrafish larvae and mice, under different light conditions.[12, 13] More recently, medicinal chemistry and screening efforts have identified a second generation of $mGlu_5$ photoswitchable NAMs. This new series includes MCS0331, which has a longer half-life in its less thermodynamically stable *cis*-isomer as compared to alloswitch-1, despite retaining similar activity as an $mGlu_5$ NAM *in vitro* and *in vivo* (Figure 1A).[13]

To date though, the molecular mechanisms behind the light-induced change of *in vitro* and *in vivo* pharmacological activity of these azobenzene-containing ligands are not well-understood and mechanistic studies investigating this are lacking. It remains under appreciated if the loss of activity of ligands is a consequence of an inability of one of the photoisomers to bind to the receptor or if it is due to more subtle changes in the binding modes of the different photoisomers that leads to changes in their ability to cause receptor activation or modulation. This aspect is markedly important as GPCR allosteric ligands can exhibit an assortment of activities, and the magnitude and type of activity they exert has implications for their ability to demonstrate *in vivo* efficacy, particularly in a context-dependent manner.[29] It is also not known whether photoswitching between the isomeric forms of the ligands can only take place when they are in the solvent and not in contact with the receptor or can also occur while the ligand is bound to the binding pocket, which may be important information when designing experiments that intend to investigate receptor function and dynamics in real-time and in a reversible manner or when trying to control rapid cellular events on a target tissue.[30]

The aim of the present study was to understand how light affects the pharmacological properties of alloswitch-1 and its analogue MCS0331, which are NAMs of $mGlu_5$ with similar *in vitro* and *in vivo* potency but have different physico-chemical properties.[12, 13] Using photochemistry and cell-based photopharmacology, we first defined the optimal wavelength and irradiance for photoisomerization of these two phenylazopyridines. Then we studied the consequences of photoisomerization on their functional activity and binding ability to $mGlu_5$, with the use of IP_1 functional assays, mass spectroscopy, radioligand binding assays and its translation to a mouse model of inflammatory pain. These data suggest that ligand bound photoisomerization takes place inside and outside the $mGlu_5$ allosteric pocket, and this drives a reversible change in affinity for these two GPCR allosteric ligands, which underlies their reversible *in vivo* activity.

Results

Photochemical properties of alloswitch-1 and MCS0331

UV-Vis spectra for each ligand (Figure 1A) were recorded in the dark and following illumination with different wavelengths of light ranging from 365 - 550 nm to reach each corresponding photostationary state (PSS; the steady state or equilibrium reached by the reversible photochemical isomerization reaction upon illumination under defined conditions with specific wavelengths and intensities) (Figure 1B). Under dark conditions, the tested azobenzene compounds exist in their *trans* isomeric form and each UV-Vis absorption spectra shows a characteristic strong π-π* transition band between 370 - 380 nm. Following illumination with different wavelengths, different PSS were obtained for the equilibrium states for *trans* to *cis* and *cis* to *trans* photoisomerization of the N=N double bond present in the azocompounds. For biological applications, we choose wavelengths that maximized the percentage of either *cis* or *trans* isomers to obtain a more pronounced biological switch under different light conditions. From these experiments, 380 nm was found to be the optimal wavelength to isomerize both alloswitch-1 and MCS0331 compounds from the extended *trans* isomer to the bent *cis* configuration. Wavelengths between 500 - 550 nm facilitated high levels of *cis*-to-*trans* photoisomerization for both allosteric NAM compounds, which is consistent with previous studies.[12, 13] The thermal relaxation in aqueous solution of the metastable *cis* isomers to the thermodinamically stable *trans* isomers was also assessed at 37ºC. The half-life of *cis*-alloswitch-1 was 26.7 seconds (s), while for *cis*-MCS0331 it was 1240 s (Figure 1C). Moreover, both compounds demonstrated robust and repetitive photochromic behavior in aqueous media for several photoisomerization cycles following 380 nm and 500 nm illumination at 37ºC (Figure 1D).

Determining the photoisomeric ratios of each PSS of a photoswitchable ligand can be critical when attempting to understand the pharmacological outcomes of a ligand and the mechanisms underlying those effects[20]. For this reason, the photoisomeric ratios of alloswitch-1 (Figure 1E top; 100% DMSO-*d6*) and MCS0331 (Figure 1E bottom; 5% DMSO-*d6* in D_2O) were determined by ^1H NMR spectroscopy, under 500 nm or 380 nm light - as determined to be the optimal photoisomerization wavelengths - at 25°C and 12°C, respectively. Different solvent and temperature conditions were tried for each compound to perform these experiments, to individually optimize responses. Under dark conditions, both compounds existed only in the thermodynamically more stable *trans* configuration. Following 500 nm illumination, 76.5% of alloswitch-1 was present in the *trans* form, and 75.2% of MCS0331 molecules existed in their *trans* form, with the remainder of molecules being present in the *cis* configuration (Figure 1E). After 380 nm illumination, 73.6% of alloswitch-1 molecules were detected in the *cis* isomeric form, whereas 80.0% of MCS0331 molecules were in the *cis* form, with the remaining molecules existing in their respective *trans* configurations (Figure 1E).

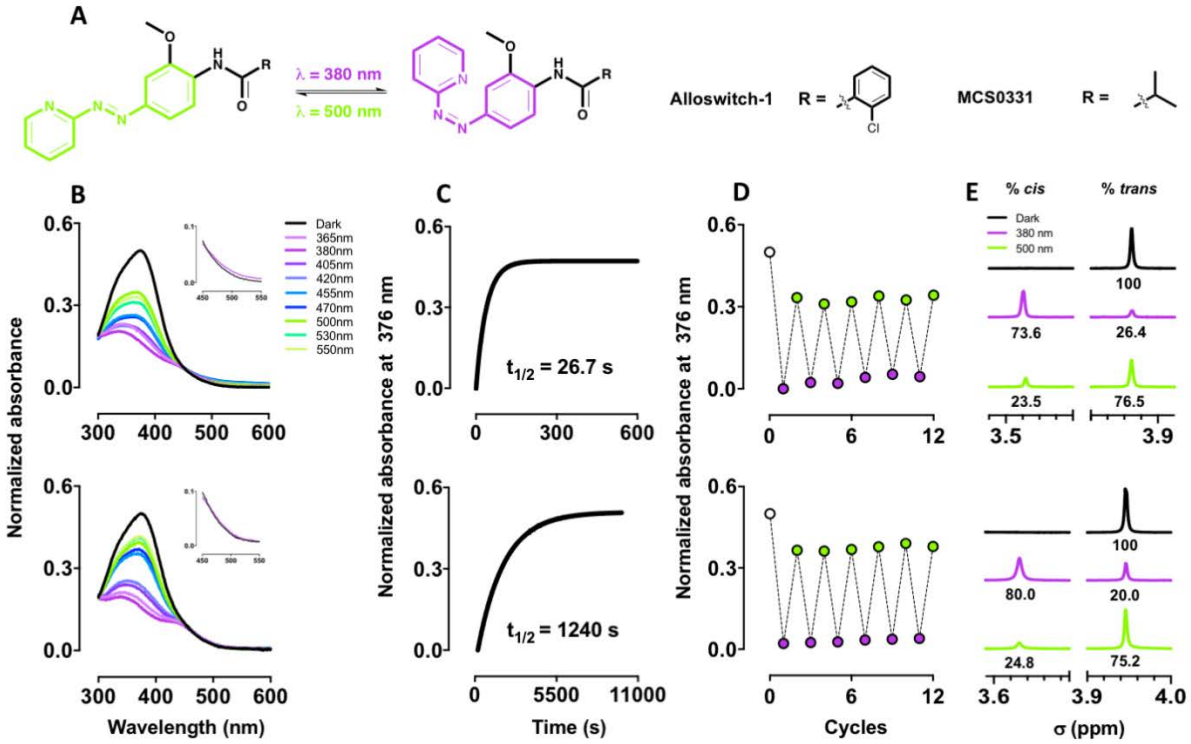

Figure 1. Chemical structure of alloswitch-1 and MCS0331 (**A**). UV-visible absorption spectra of 30 μM alloswitch-1 (**B; top**) and MCS0331 (**B; bottom**) following continuous illumination with different wavelengths of light (details in methods section) or dark conditions in 3% DMSO binding buffer, pH 7.5. Inset graphs highlights the absorption between 450 and 550 nm for alloswitch-1 (**B; top)** and for MCS0331 (**B; bottom)**. Thermal relaxation of 30 μM alloswitch-1 (**C; top**) and 30 μM MCS0331 (**C; bottom**), following continuous illumination with 380 nm, in 3% DMSO, binding buffer, pH 7.5 at 37ºC. Reversibility and stability of photoisomerization of 5 μM alloswitch-1 in binding buffer containing 5% DMSO, pH 7.5 (**D; top**) and 30 μM MCS0331 in 3% DMSO binding buffer, pH 7.5 (**D; bottom)** following continuous illumination with 380 nm or 500 nm. Representative ^{1}H-NMR spectra of (**E; top**) alloswitch-1 (1 mM) in DMSO-*d6* and (**E; bottom**) MCS0331 (500 μM) in 5% DMSO-*d6* in D_2O following either dark conditions or 3 min of continuous illumination with 380 nm or 500 nm at 25ºC and 12ºC, respectively. All absorbance data were normalized between 0 – 0.5 (**B, C, D**).

Fine-tuning wavelength and irradiance for photoswitching of $mGlu_5$ NAM biological activity

The effects of wavelength and irradiance on the ability of alloswitch-1 and MCS0331 to act as NAMs were studied in the canonical $G_{q/11}$-linked inositol phosphate (IP_1) accumulation assay in HEK 293 cells transiently transfected with the human (h)$mGlu_5$ receptor (Figure 2). The change in pIC_{50} values reported for these interactions between photoswitchable NAMs and the test agonist provides information about the photoswitching efficiency of the ligands; where the larger the difference in potency between light conditions, the more efficient the photoswitching of the

ligand between its isomeric states.[13] In agreement with previous reports, both alloswitch-1 (Figure 2A, C) and MCS0331 (Figure 2B, D) completely inhibited the IP_1 response induced by a single, fixed concentration of quisqualate (100 nM) under dark conditions (pIC_{50} values of 7.64 ± 0.06 and 7.46 ± 0.07, respectively, Figure 2A, B, C, D) indicative of strong negative cooperativity between the allosteric ligands and quisqualate.[12, 13] Following illumination with different wavelengths, the largest change in pIC_{50} values from dark conditions for either alloswitch-1 or MCS0331 were observed for wavelengths in the 365 nm - 420 nm range, and there were no significant differences between these values (Figure 2E). Thus, 380 nm light was selected for promoting *trans*-to-*cis* photoisomerization of the phenylazopyridines for the remainder of the experiments, while illumination with 500 nm was chosen to promote *cis*-to-*trans* photoisomerization of the phenylazopyridines.

In order to determine the optimal light intensity for photoswitching from *trans*-to-*cis* isomeric forms, each photoswitchable NAM was interacted with 100 nM of quisqualate under 380 nm conditions, with different irradiances ranging from 0 to 0.15 mW/mm^2 (Figure 2C, D, F). Values from 0.10 mW to 0.15 mW/mm^2 demonstrated the greatest pharmacological potency change for NAMs, but were not significantly different. For this reason, wavelength irradiance was set to 0.12 mW/mm^2. Interestingly, the change in potency for each interaction at different wavelengths and irradiances appeared to reach a limit, where no further changes in potency could be seen for that interaction under those conditions, indicative of the system reaching a PSS at a given wavelength and intensity. The data from Figure 2F also suggest that, when a system has insufficient time to reach a PSS, the light power can influence the rate at which a photoswitchable ligand can photoisomerize (and reach a PSS), as is reflected in the differences in the ligand potency values with changing light power.

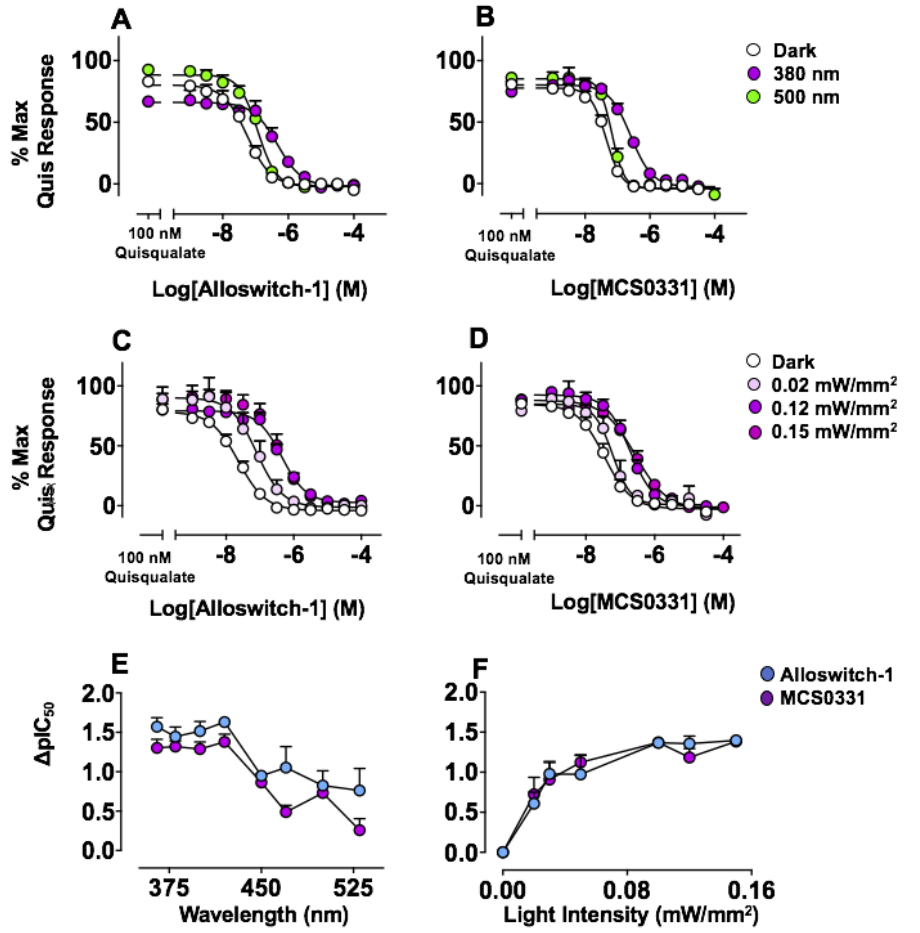

Figure 2. Effects of wavelength and irradiance on alloswitch-1 and MCS0331 negative allosteric modulation of $mGlu_5$. In IP_1 accumulation assays the effect of different wavelengths of light (irradiance at 0.12 mW/mm^2) on the ability of alloswitch-1 (**A**) or MCS0331 (**B**) to inhibit the functioning of an EC_{80} concentration of quisqualate (100 nM) was assessed at the $hmGlu_5$. The ability of different irradiances of the 380 nm on alloswitch-1 (**C**) or MCS0331 (**D**) modulation of 100 nM quisqualate was also investigated. The change in pIC_{50} values between dark and light conditions for each interaction was determined following illumination with different wavelengths of light (**E**) or illumination at 380 nm with variable irradiances (**F**). Data represent the mean ± SEM of at least three independent experiments performed in duplicate.

Photoswitchable negative allosteric modulation of agonist-induced IP_1 accumulation

In order to quantify functional affinity and cooperativity estimates in IP_1 accumulation assays, NAM interactions with agonists were fitted to an operational model of allosterism.[31] In all cases, the functional affinity for orthosteric agonists were constrained to values determined in separate IP_1 accumulation assays; where cells were transfected with different amounts of $hmGlu_5$ receptor, and under dark, 500 nm or 380 nm conditions agonist concentration-response curves were generated (Supplementary Figure 1). By fitting the resulting curves to the operational model

of agonism, it was determined that both the functional affinity and operational efficacy estimates generated for either glutamate or quisqualate were unaffected by the light conditions, which is consistent with the activity of these ligands being independent of light (glutamate pK_A = 4.51 – 4.60, glutamate τ = 1.41 – 2.0; quisqualate pK_A = 7.26 – 7.65, quisqualate τ = 1.17 – 1.55; Supplementary Table 1).[32, 33] For interaction studies with NAMs, under dark or 500 nm conditions, the functional affinity estimates for alloswitch-1 and MCS0331 were in the range of pK_B = 6.87 – 8.04 and pK_B = 7.43 – 8.65, respectively (Table 1). Under these conditions and at the concentrations tested, both alloswitch-1 and MCS0331 behaved as NAMs of agonist-mediated IP_1 accumulation (alloswitch-1 Logβ = -0.62 – -1.25; MCS0331 Logβ = -0.97 – -1.35, Figure 3; Table 1). Both NAMs had a trend for higher negative cooperativity with quisqualate activity than with glutamate at the $mGlu_5$ and their functional affinity estimates were reduced under 500 nm conditions as compared to dark conditions, with the exception of the interaction between MCS0331 and glutamate, which resulted in equivalent functional affinity estimates between dark and 500 nm conditions (Figure 3, Table 1).

Following 380 nm irradiation, both ligands had reduced functional affinity for the receptor, regardless of the interacting orthosteric probe (Table 1). They also showed minimal differences in their negative cooperativity with glutamate activity and only a small reduction in negative cooperativity with quisqualate; this change though, was not substantial (Figure 3C, F, I, L; Table 1). Taken together, these data indicate that the major mechanism underling the change in activity of alloswitch-1 and MCS0331 from dark to 380 nm conditions is due to a loss in affinity for the $mGlu_5$ rather than a change (or switch) in cooperativity, whereby the *cis* isomers of the phenylazopyridines may no longer be able to bind to the allosteric pocket of the receptor or they bind to a lower affinity site on the receptor.

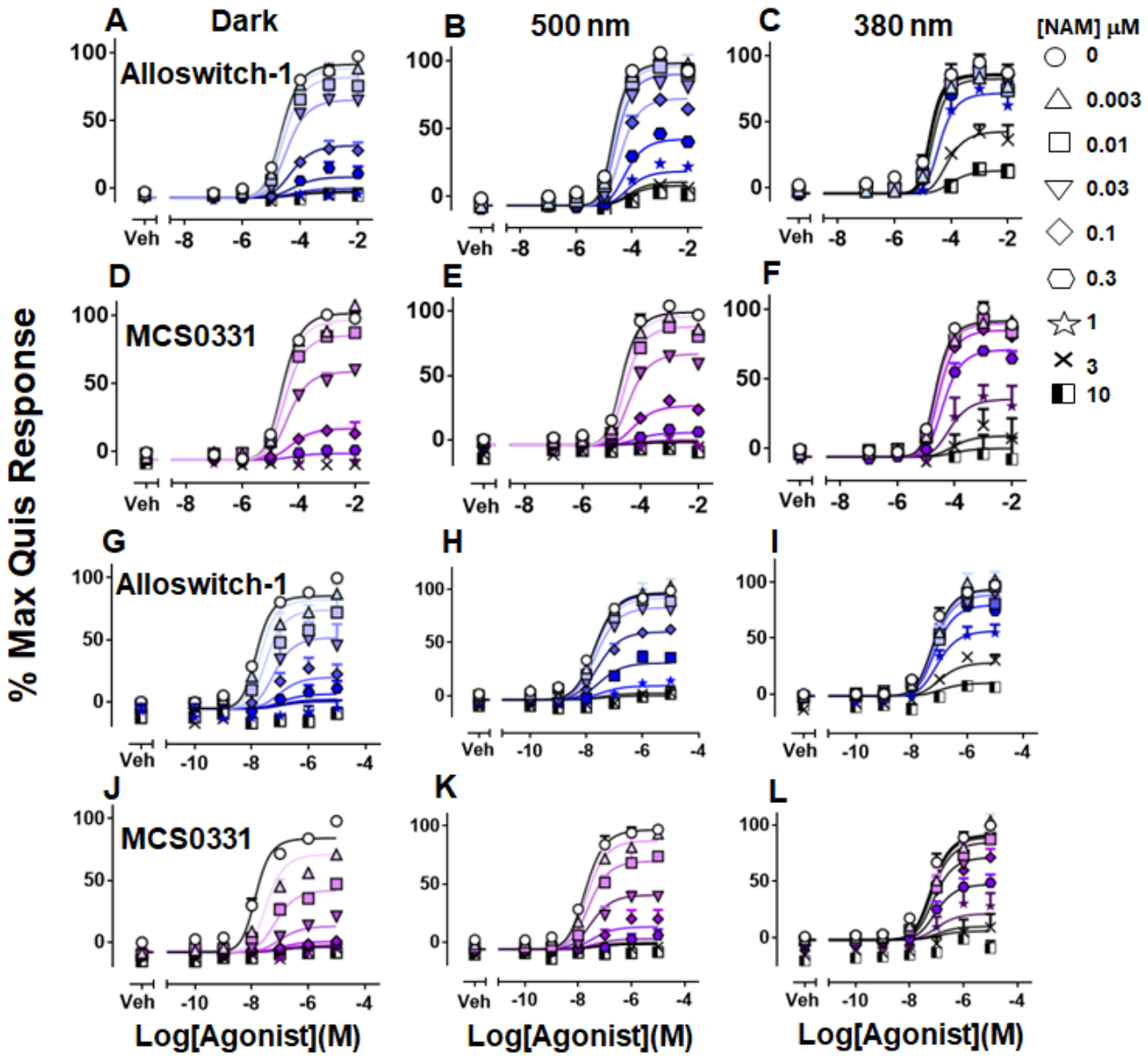

Figure 3. Effect of light on the ability of the $mGlu_5$ NAMs, alloswitch-1 (A-C, G-I), or MCS0331 (D-F, J-L), to negatively modulate glutamate (A-F) or quisqualate (G-L)-stimulated IP_1 accumulation in HEK cells transiently transfected with $hmGlu_5$. Data are expressed as a % of maximal quisqualate response, as determined by a fixed concentration of quisqualate (quis; 10 μM), and represent the mean ± SEM of at least three independent experiments performed in duplicate. Fitted curves are from global analysis of datasets according to Equation 1 (in Supplementary Methods), with appropriate constraints and parameter estimates are shown in Table 1, results and methods.

Table 1. Operational model estimates for the interactions between alloswitch-1 or MCS0331 with the indicated othosteric agonist and light condition in IP_1 accumulation assays in $hmGlu_5$ expressing HEK cells.

Allosteric ligand	Dark				500 nm				380 nm			
	+ glutamate		+ quisqualate		+ glutamate		+ quisqualate		+ glutamate		+ quisqualate	
	[a]pK_B	[b]Logb (b)	[a]pK_B	[b]Logb (b)	[a]pK_B	[b]Logb (b)	[a]pK_B	[b]Logb (b)	[a]pK_B	[b]Logb (b)	[a]pK_B	[b]Logb (b)
Alloswitch-1	7.34 ± 0.07	-0.97 ± 0.11 (0.11)	8.04 ± 0.09	-1.25 ± 0.10 (0.06)	6.97 ± 0.06	-0.62 ± 0.03 (0.24)	6.87 ± 0.07	-1.23 ± 0.24 (0.06)	5.96 ± 0.14	-0.81 ± 0.13 (0.15)	5.88 ± 0.23	-0.89 ± 0.11 (0.13)
MCS0331	=7.50[$]	-1.16 ± 0.13 (0.07)	8.65 ± 0.05	-1.35 ± 0.08 (0.04)	7.43 ± 0.06	-0.97 ± 0.10 (0.11)	7.75 ± 0.07	-1.08 ± 0.14 (0.08)	6.39 ± 0.09	-0.93 ± 0.13 (0.12)	6.54 ± 0.11	-0.75 ± 0.17 (0.18)

[a]Negative logarithm of the allosteric modulator equilibrium dissociation constant.

[b]Logarithm of the efficacy scaling factor (antilog values shown in parentheses) for the effect of the indicated NAM on agonist responses under different light conditions; when the logarithm of the affinity cooperativity between the agonist and the NAM is equal to zero ($\log\alpha = 0$), it is equivalent to the combined functional cooperativity between ligands ($Log\alpha\beta$). Combined cooperativity values with a corresponding $ were derived from applying an absolute sum of squares analysis.

Estimated parameters represent the mean ± SEM of at least three experiments performed in duplicate. Functional IP_1 accumulation responses were analyzed according to Equation 1.

Photoswitchable control of affinity and dissociation kinetics of $mGlu_5$ ligands by MS binding

To further understand the mechanisms of modulation of alloswitch-1 and MCS0331, MS binding studies under dark, 500 nm and 380 nm conditions were undertaken on membranes expressing $mGlu_5$ (Figure 4). The advantage of utilizing the MS binding technique over more conventional radioligand binding assays is that it allows for the quantification of affinity estimates from the direct binding of a ligand of interest to its target without the need of a competing radioligand. In saturation binding assays and under dark and 500 nm conditions, the equilibrium dissociation constants for alloswitch-1 and MCS0331 were $pK_{D(dark)}$ = 7.51 ± 0.04 and $pK_{D(500)}$ = 7.47 ± 0.07 and $pK_{D(dark)}$ = 7.85 ± 0.03 and $pK_{D(500)}$ = 7.58 ± 0.06, respectively (Table 2). For experiments performed under 380 nm conditions, when phenylazopyridines exist mostly in their *cis* form, the equilibrium dissociation constants for alloswitch-1 and MCS0331 were significantly augmented as compared to dark conditions (alloswitch-1 $pK_{D(380)}$ = 7.03 ± 0.05 and MCS0331 $pK_{D(380)}$ = 6.90 ± 0.10). These results support the IP_1 accumulation data which suggest that there is a robust change in the affinity of alloswitch-1 and MCS0331 from dark to 380 nm conditions, and this may underly the change in the functional potency of these ligands.

We used the observed photoisomeric ratios of alloswitch-1 and MCS0331 determined by ^{1}H-NMR (Figure 1E) to resolve if a reduction of the concentration of active *trans* isomer is sufficient to account for the change in observed affinity of each ligand, between light conditions. By making the assumption that the *trans* isomer of the phenylazopyridines is the only species that binds to the receptor and has functional activity, it is possible to correct the concentrations reported in the binding assays, under different light conditions, to only account for the *trans* isomer and, then, to compare the adjusted affinity value with that reported in Table 2 for assays performed under

dark conditions (i.e. where only *trans* isomer is present). By simulating this with the alloswitch-1 380 nm saturation binding dataset, a corrected *trans*-alloswitch-1 equilibrium dissociation constant was determined to be pK_D = 7.58 ± 0.08, which is not significantly different from the pK_D reported for alloswitch-1 under dark conditions, as determined by one-way ANOVA (Table 2). This suggests that the change in the reported pK_D values between dark and 380 nm conditions could be explained by a dilution effect of the active *trans* species and a reduced binding of the *cis* isomer. Similarly, by applying the same simulation to the MCS0331 dataset, we found that the change in the reported pK_D values from dark to 380 nm conditions could also be explained by a dilution effect of *trans*-MCS0331 - by correcting the MCS0331 concentration in the 380 nm dataset a new equilibrium dissociation constant was generated to be pK_D = 7.60 ± 0.10, which is not significantly different from the pK_D reported for MCS0331 under dark conditions (Table 2).

To determine if *cis* isomer binding of ligands is possible and if photoisomerization can take place within the $mGlu_5$ binding pocket, in addition to appreciating which factors may contribute to the affinity change of these ligands at the $mGlu_5$, MS dissociation kinetic assays were also performed with the phenylazopyridines following dark, 500 nm or 380 nm conditions. Under dark conditions, the dissociation rate of MCS0331 for its binding site was slower than alloswitch-1, which could, in part, explain the improved affinity and potency of MCS0331 in the IP_1 accumulation assay as compared to alloswitch-1 (Figure 4C, D; Table 3). Following 500 nm or 380 nm irradiation after an incubation in the dark, the dissociation rates of both alloswitch-1 and MCS0331 were significantly increased as compared to dark conditions (Figure 4C, D; Table 3). These data suggest that the decreased affinity of either alloswitch-1 or MCS0331, under 380 nm conditions, is in part due to ligands in the *cis* configuration binding to the receptor and dissociating at a faster rate than their respective *trans* isomers. The data also support the concept that photoswitching between isomeric forms of the ligands can occur inside the $mGlu_5$ allosteric pocket. Since the association phase is performed under dark conditions to allow for *trans* isomer binding, the initiation of the dissociation phase under 380 nm conditions would then suggest that *trans*-to-*cis* photoisomerization of ligands within the allosteric pocket is possible - given that the observed dissociation rate is significantly faster (Figure 4C, D). Additional MS dissociation kinetic assays were also performed with MPEP as a control to show that its dissociation rate was minimally affected by light (Figure S3; Table S4).

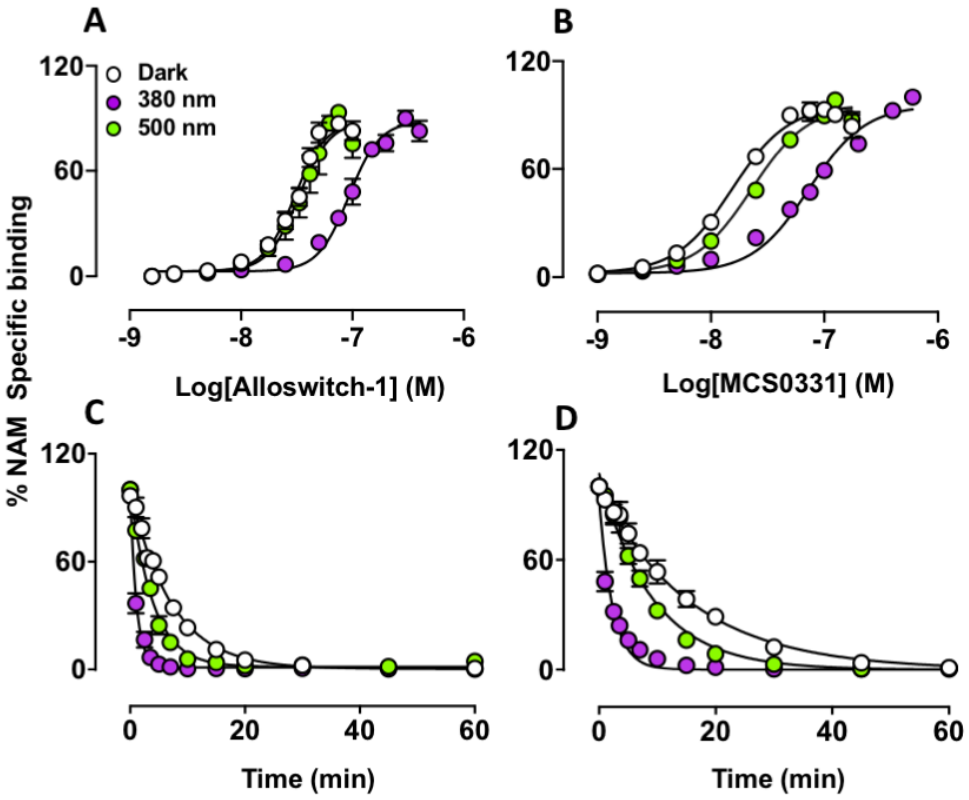

Figure 4. Effect of light on alloswitch-1 and MCS0331 affinity and dissociation kinetics as determined by MS binding assays. For MS saturation experiments (**A, B**), $mGlu_5$ expressing membranes were incubated with increasing concentrations of marker ligand for 1h at 37ºC under different light conditions. For dissociation kinetic experiments (**C**) 32 nM of alloswitch-1 or (**D**) 15 nM of MCS0331 was incubated with $mGlu_5$ expressing membranes for 1h at 37ºC, under dark condition, and dissociation half-lives (Table 3) were determined by the addition of a saturating concentration of the competitive NAM, VU409106, at different time points and under different light conditions. Data are expressed as a percentage of specific binding and represent the mean ± SEM of at least three independent experiments performed in duplicate.

Table 2. Summary of photoswitchable NAM affinities and B_{max} estimates under different light conditions as determined by MS binding assays.

	Dark		500 nm		380 nm	
Allosteric ligand	**[a]pK_D**	**[b]B_{max} (pmol/mg protein)**	**[a]pK_D**	**[b]B_{max} (pmol/mg protein)**	**[a]pK_D**	**[b]B_{max} (pmol/mg protein)**
Alloswitch-1	7.51 ± 0.04	71.52 ± 6.89	7.47 ± 0.07	76.34 ± 13.98	7.03 ± 0.05****	35.06 ± 11.68
MCS0331	7.85 ± 0.03	92.84 ± 9.92	7.58 ± 0.06*	151.51 ± 16.28	6.90 ± 0.10****	21.06 ± 2.05

[a]Negative logarithm of the allosteric modulator equilibrium dissociation constant.

[b]Receptor expression of $hmGlu_5$.

Datasets were analysed according to Equation 2.

Difference in equilibrium dissociation constants of allosteric ligands under different light conditions were determined by one-way ANOVA, and Tukey post hoc test where appropriate. *P< 0.1 and ****P< 0.0001 vs dark light conditions.

Table 3. Summary of photoswitchable NAM dissociation kinetic parameters estimates under different light conditions as determined by MS binding assays.

	Dark		500 nm		380 nm	
	[a]k_{off} (min^{-1})	**[b]$t_{1/2}$ (min)**	**[a]k_{off} (min^{-1})**	**[b]$t_{1/2}$ (min)**	**[a]k_{off} (min^{-1})**	**[b]$t_{1/2}$ (min)**
Alloswitch-1	0.14 ± 0.01	5.04 ± 0.10	0.25 ± 0.01*	2.77 ± 0.14	0.93 ± 0.16****	0.81 ± 0.15
MCS0331	0.07 ± 0.01	10.70 ± 0.95	0.11 ± 0.01*	6.32 ± 0.29	0.47 ± 0.07****	1.61 ± 0.28

[a]Dissociation rate of the indicated NAM.

[b]$t_{1/2}$ is the half-life of dissociation.

Difference in the dissociation rate was determined by one-way ANOVA, which is performed on the logarithm of the k_{off} values. *P< 0.1 and ****P< 0.0001 vs dark light conditions for 500 nm and 380 nm light condition, respectively.

Effects of interacting photoswitchable NAMs with [^{3}H]-MPEP in radioligand binding assays

Previous computational docking and MD studies have suggested that alloswitch-1 may bind deep within the common MPEP allosteric pocket of $mGlu_5$ seven transmembrane domain (7TM) and experimental studies show that alloswitch-1 NAM activity is affected following mutation to either S809 or the P655 residue, which also effect MPEP activity.[30] Thus, [^{3}H]-MPEP radioligand binding studies were performed with membranes prepared from $mGlu_5$-HEK293 cells to determine if alloswitch-1 and/or MCS0331 share a common/overlapping binding site with [^{3}H]-MPEP, in addition to determining the cooperative effects of NAMs on agonist binding alone (α), under different light conditions (Figure 5).

[^{3}H]-MPEP bound to $mGlu_5$-membranes in a monophasic and saturable manner with an estimated pK_D = 8.40 ± 0.009 and maximal binding capacity of (B_{max}) of 1777 ± 72.05 fmol/mg of protein under dark conditions and these estimates were not significantly affected by changing light conditions (data not shown). Under dark light conditions, both alloswitch-1 and MCS0331 completely inhibited the specific binding of a fixed concentration of [^{3}H]-MPEP (~10 nM) indicative of NAMs binding to or overlapping with the common MPEP binding site (Figure 5). Furthermore, there was no difference between the apparent binding affinity estimates for either alloswitch-1 or MCS0331 between dark (alloswitch-1 pK_D = 7.91 ± 0.11; MCS0331 pK_D = 8.33 ± 0.07) and 500 nm conditions (alloswitch-1 pK_D = 7.92 ± 0.08; MCS0331 pK_D = 8.03 ± 0.08), but the apparent binding affinities of NAMs were reduced for 380 nm conditions (alloswitch-1 pK_D = 7.16 ± 0.05; MCS0331 pK_D = 6.59 ± 0.10), which is consistent with both the IP_1 accumulation and MS binding data.

In order to evaluate the effect of agonist binding to the orthosteric site on NAM binding to the [^{3}H]-MPEP allosteric site, [^{3}H]-MPEP competition binding studies were repeated in the absence or presence of an orthosteric site-saturating concentration of either glutamate (1 mM) or quisqualate (30 μM).[34, 35] Incubation of glutamate or quisqualate with [^{3}H]-MPEP alone had no effect on the specific binding of [^{3}H]-MPEP (data not shown), and the apparent binding affinities of alloswitch-1 or MCS0331 were also unaffected by the presence of either 1 mM glutamate or 30 μM quisqulate, under dark or 500 nm conditions, as determined by F-test (Figure 5). Following 380 nm irradiation though, there was a small difference in the apparent affinity estimates of both NAMs in the presence of either agonist (ΔpK_I = 0.26 – 0.31; $P<0.05$ F-test; Figure 5). Since the concentrations of agonist used in these experiments fully occupies the orthosteric site, any observed change in the apparent binding affinity of NAMs in the presence or absence of agonist would reflect the degree of affinity cooperativity (α) between the respective interacting agonist/NAM pairs. These data then suggest that there is very limited to negligible affinity cooperativity existing between NAM and agonist interacting pairs at the $mGlu_5$ under all light conditions.

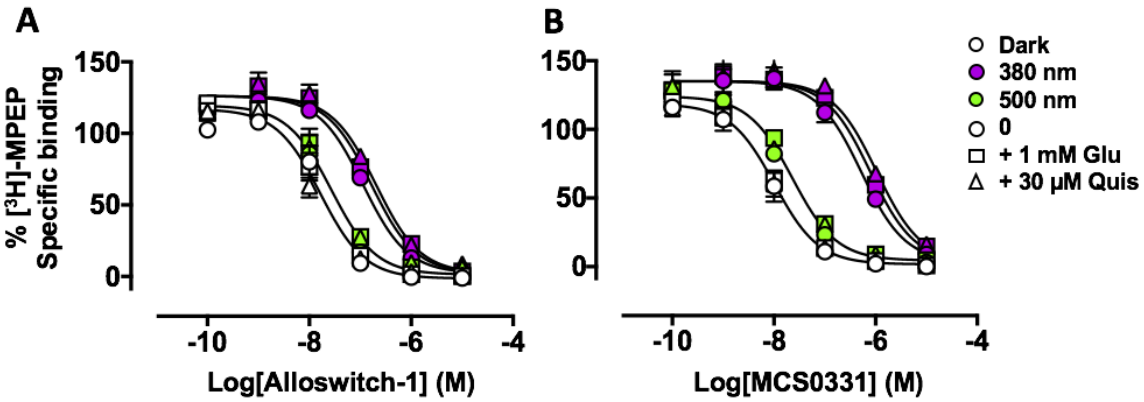

Figure 5. [^{3}H]-MPEP competition radioligand binding studies to demonstrate the effect of either a saturating concentration of glutamate (1 mM glu) or quisqualate (30 µM quis) on alloswitch-1 (A) or MCS0331 (B) - mediated inhibition of [^{3}H]-MPEP binding in hmGlu$_5$ expressing membranes. Data are expressed as a percentage of specific binding and represent the mean ± SEM of at least three independent experiments performed in duplicate. Fitted curves are from global analysis of datasets according to Equation 3 (in Methods) with parameter estimates shown in text.

Reversible loss of NAM effect through photoisomerization translates *in vivo*

Considering the mechanisms of action of these photoswitchable NAMs, it was of interest to determine how their *in vitro* activity is translated *in vivo*. To that aim, we tested the photoswitchable mGlu$_5$ NAMs in a preclinical mouse model of inflammatory pain in which MPEP, a prototypical mGlu$_5$ NAM, has historically shown efficacy following local injection in the amygdala (Figure 6). [36]

Prior to testing though, the ability of alloswitch-1 and MCS0331 to negatively modulate glutamate function at the mouse mGlu$_5$, under dark, 500 nm or 380 nm conditions, was firstly confirmed since some allosteric ligands can show species differences. Both ligands negatively modulated the effects of glutamate to similar extents to that seen for their modulation at the human orthologue, while the activity of the prototypical mGlu$_5$ NAM, MPEP, was unaffected by light (Supplementary Figure 5 and Supplementary Table 4).

Mice were stereotaxically implanted with hybrid optic and fluid cannulas into the amygdala to enable the controlled release of compound and light. Mice were then injected with CFA into the left hind paw to induce persistent inflammatory pain. The effect of intra-amygdala injection of either vehicle, MPEP, alloswitch-1 or MCS0331 on the mechanical pain threshold of animals was then assessed by stimulating the CFA-treated paw with von Frey filaments (eight days after CFA injection; Figure 6). On test day (day 8), intra-amygdala injection of MPEP, but not vehicle, returned mechanical sensitivity to the level of naive mice (or before inflammation was induced; Figure 6 and Supplementary Figure 6) and these effects were independent of light. Following injection of either alloswitch-1 or MCS0331, under dark conditions, the mechanical pain threshold of animals was also restored (Figure 6). This

analgesic effect of photoswitchable NAMs was lost after intra-amygdala illumination with 385 nm and then restored with 505 nm illumination. This indicates that the loss in affinity of each phenylazopyridine for the $mGlu_5$, following local *trans*-to-*cis* photoisomerization within the amygdala (both inside and outside the binding pocket) leads to insufficient levels of receptor occupancy for the phenylazopyridines to have an analgesic effect on mechanical pain, under 380 nm conditions. An effect that can be reversed by local 505 nm irradiation, and *cis*-to-*trans* photoisomerization of ligands to their higher affinity states. This reversible behavior was not observed with MPEP, consistent with it behaving as a non-photoswitchable $mGlu_5$ NAM in cell-based assays. These data are also consistent with previous *in vivo* results that have shown alloswitch-1 and MCS0331 to have reversible, analgesic properties in mouse models of pain, and so do further support the potential for using photoswitchable $mGlu_5$ NAMs to investigate the role of the $mGlu_5$ in pain in a more spatiotemporal manner.[13] More broadly speaking, they also outline the potential use of photoswitchable ligands to investigate receptor function in other disease contexts in a more dynamic way.

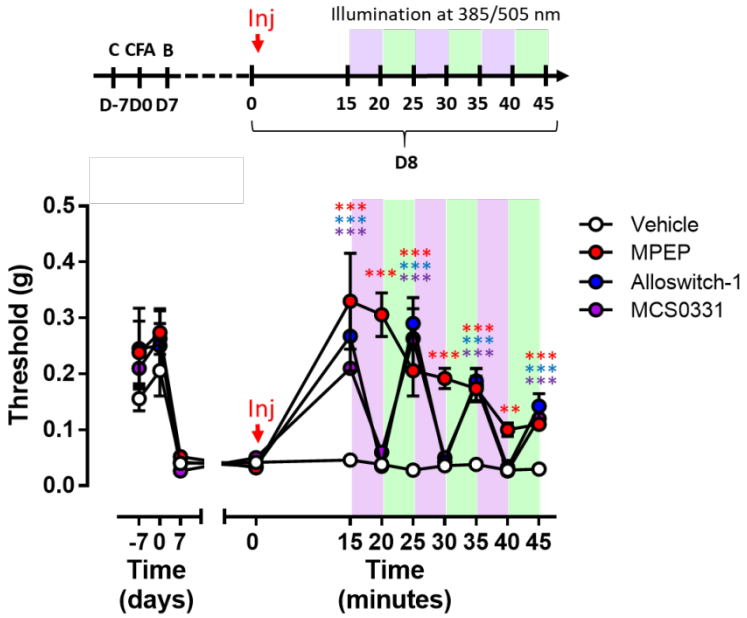

Figure 6. Light-dependent antiallodynic effect of Alloswitch-1 and MCS0331 in a mouse model of inflammatory pain. Persistent inflammatory pain was induced in mice by injection of complete Freund's adjuvant (CFA) into the left hind paw of mice on day 0 (D0) of timeline. In the timeline of experiment, "C" refers to the day of intra-amygdala cannulation, "CFA" refers to day of CFA injection, "B" refers to day of pre-test baseline reading. The mechanical pain threshold of animals was evaluated by stimulating the CFA-treated hind paw of animals with von Frey filaments. The mechanical sensitivity of naive animals was measured prior to cannulation, then prior to CFA injection and 7 days after (left-segment of figure). On test day, 8 days after CFA injections (D8; right-segment of figure), the mechanical sensitivity of animals was tested (t0) immediately after they received an intra-amygdala injection of either vehicle (n = 5), MPEP (1 μM; n = 5), alloswitch-1 (300 nM; n = 4) or MCS0331 (300 nM; n = 3).

The effect of each treatment was assessed after 15 minutes (without light) then every 5 minutes following intra-amygdala illuminations (protocol: 50 ms light pulses at 10 Hz frequency for 5 minutes) at 385 nm (irradiance: 0.11 mW/mm^2) or 505 nm (0.029 mW/mm^2). Data were analysed by two-way ANOVA and expressed as mean ± SEM, $^{**}P < 0.01$ and $^{***}P < 0.001$ denotes significant difference on mechanical pain threshold of drug treated-animals as compared to vehicle for each time point.

Discussion

The $mGlu_5$ is an exemplar class C GPCR and represents an important therapeutic target for CNS disorders. Light control of GPCRs, including the $mGlu_5$, through photopharmacology is emerging as an interesting approach for achieving improved functional selectivity and spatiotemporal control over drug actions at their targets, in addition to enhancing our understanding of receptor function and dynamics. Since the field of photopharmacology is in its early stages of development, there are currently limited studies available that have explored the mechanisms of action of photoswitchable allosteric ligands for GPCRs. For instance, alloswitch-1 and MCS0331 are two $mGlu_5$ photoswitchable allosteric modulators that can reversibly inhibit the functional effects of a fixed concentration of agonist, depending on the light conditions used, but relatively little is known about their mechanism of action/modulation at the $mGlu_5$.[12, 13] For this reason, our study has investigated the functional and binding consequences of alloswitch-1 and MCS0331 under different light conditions at the $mGlu_5$ using canonical $G_{q/11}$-linked signalling assays (IP_1 accumulation), MS binding and radioligand binding assays. This study has also characterized the wavelengths and light intensities at which the phenylazopyridines can photoswitch between their isomeric states and so has fine-tuned *in vitro* conditions to promote efficient photoswitching of ligands, which could potentially be extended to similar experimental photopharmacology set ups.

In terms of photochemistry, this study has shown that, despite alloswitch-1 and MCS0331 sharing a common scaffold and similar electronic features, each compound has distinct photochemical properties. Alloswitch-1 has a shorter *cis*-to-*trans* thermal relaxation half-life as compared to MCS0331 and the *cis*-MCS0331 n-π* transition band is more intense than that of *cis*-alloswitch-1. These differences may be explained by the electron delocalization through the central ring and the chlorophenyl of alloswitch-1, which is not present in the aliphatic carboxamide of MCS0331. Importantly, these differences in photochemistry contribute to the differences observed in each ligands' photopharmacology and should be considered when performing pharmacological assays. Photochemical experiments, in this study, were performed under the most appropriate (solvent, concentration and temperature) conditions found to allow for the accurate estimation of half-lives and PSSs values for each compound under each light condition tested. It should be noted though, that the resulting parameter estimates may not be fully representative of the half-lives and PSSs values expected for each phenylazopyridine, when tested in the pharmacological assays, which employ more physiologically relevant conditions (including aqueous, buffered solutions and the presence of the $mGlu_5$). For this reason, photochemical estimates generated in this study have

only been used as a guide to aid the interpretation of the pharmacological data under different light conditions. This also highlights the important need for improved photoswitchable ligands with appropriate physical and photochemical properties (e.g. suitable solubility and slow relaxation times) for pharmacological and biological applications.

In functional assays, alloswitch-1 and MCS0331 are potent NAMs of agonist-induced IP_1 accumulation; NAMs reduce agonist potency and maximum response at the $mGlu_5$, under dark or 500 nm conditions. While following 380 nm irradiation, the pheylazopyridines have reduced NAM activity with agonist-induced IP_1 accumulation, which is consistent with previous reports.[12, 13] Functional operational estimates indicate that this switch in activity is overall due to a loss in allosteric ligand affinity, rather than a substantial change in cooperativity between interacting ligands.

To understand this in more detail, MS binding data generated under different light conditions were considered in the context of the photoisomeric ratio of each NAMs' PSSs. These data suggest that the $mGlu_5$ affinity of both alloswitch-1 and MCS0331 following 500 nm or 380 nm irradiation is reduced, as compared to those estimates obtained under dark conditions. Given the mixed population of *trans* and *cis* ligands existing under irradiated conditions and, when considering the equilibrium binding data in isolation, these observed differences in binding parameters could be explained by a reduction in the available *active trans* isomer concentration, and a lack of *cis* isomer receptor binding. It then follows that the potential inability of the *cis* form of the phenylazopyridines to bind to the receptor may underpin the loss in functional NAM activity observed in the IP_1 accumulation assay, following UV light conditions. For this reason, the MS dissociation kinetic data provide further insight into the binding capabilities of these ligands. Since, the dissociation rate constants of ligands were significantly faster under irradiated conditions this suggests that *cis*-to-*trans* photoisomerization is possible within the binding pocket and that the *cis* isomer of ligands are capable of binding to the receptor, albeit with reduced affinity and a shorter residence time (given the faster dissociation rates from the receptor), when compared to the *trans* isomers. This idea is in line with the hypothesis proposed by Dalton et al., (2016), who suggested that photoswitching between isomeric forms could theoretically occur while alloswitch-1 is bound to the allosteric pocket.[24] It is though possible that differences in the association rates of each isomeric form of ligands for the receptor may also affect the affinity of these ligands. There is increasing evidence that indicates that the association rates of drugs are not diffusion limited and so, in addition to dissociation rates, association rates can also impact the determination of affinity and the pharmacological profile of drugs in different disease contexts.[37, 38] Since receptor binding is a dynamic process, a decreased association rate may also impact the ability of a molecule to rebind to a (nearby) receptor following its dissociation into the local environment before it finally diffuses away or is metabolized.[37] In this regard, both association and dissociation rates are likely to be important to the mechanism of action of these photoswitchable allosteric ligands.

Additional radioligand binding studies confirmed that the active *trans* configuration of the phenylazopyridines bind to the common MPEP binding site since they completely inhibit [^{3}H]-MPEP specific binding, where the hillslopes were ~1, indicative of a single binding site. Since the apparent affinity estimates of photoswitchable NAMs were not changed (or there were only slightly affected) by the addition of an orthosteric-site saturating concentration of either glutamate or quisqualate, it is also suggested that the major mechanism for modulating the activity of an orthostheric agonist is through modulating its intrinsic efficacy and not binding affinity. The ability of alloswitch-1 and MCS0331 to behave as NAMs of agonist signaling efficacy but not agonist binding affinity, is consistent with the mechanisms of other class C $mGlu_1$ and $mGlu_5$ NAMs, including CPCCOEt and MPEP.[34, 39] This suggests that this could be a common mechanism by which NAMs modulate agonist activity at group I mGlu receptors. Our study also implies that there is little probe dependent behavior for alloswitch-1 and MCS0331 with respect to the activity of orthosteric full agonists at the $mGlu_5$, as they regulate the activity of glutamate and quisqualate by similar mechanisms.

These data, in consideration with the previous computational study by Dalton et al., (2016), support the notion that *trans* phenylazopyridines bind deep into the transmembrane of $mGlu_5$, exploiting in part the MPEP binding pocket where they stabilize a water molecule mediated hydrogen-bond network in the bottom of the pocket through connections with residues on TM3, TM6 and TM7 (including residue S809 in TM7, which $mGlu_5$ prototypical NAMs commonly interact with).[30, 40, 41] Through these interactions, it is hypothesized that *trans* phenylazopyridines stabilize a NAM-induced inactive state of the receptor that promotes the transmission of negative cooperativity between the allosteric and orthosteric sites of the receptor.[30] Following *trans*-to-*cis* photoisomerization inside (or outside) the allosteric pocket, we along with Dalton et al., (2016), predict that the ligands, in their *cis* configuration, can no longer stabilize this network or interact with residue S809 or P655, and instead we hypothesize that they rapidly dissociate from the receptor.[30] When bound in this position, *cis* ligands may undergo a molecular switch; no longer binding as tightly to the receptor or engaging residues important for NAM activity. Although, we cannot exclude the possibility of differences in association rates of the *cis* isomer of ligands also impeding their ability to bind to the receptor.

Molecular switches have been well-documented for allosteric ligands at the $mGlu_5$, in addition to ligands of other mGlu receptors, and have made the development of structure-activity relationships around $mGlu_5$ allosteric ligands notoriously difficult and superficial.[42-46, 40] Future mutational, computational and structural studies that utilize a constrained version of *cis*-alloswitch-1 and *cis*-MCS0331, which cannot isomerize back to its active NAM form, may however, be necessary to shed further understanding on the binding modes of these photoswitchable allosteric ligands, and to identify other key residues important to driving their activity between isomers.

An important consideration when interpreting these data and a limitation to this study is that the dynamic interconversion of the phenylazopyridines between their isomers - induced by photon absorption - occurs faster

than biological events at the $mGlu_5$. A molecule may switch many times between isomers, not only when bound or unbound, but also while (un)binding to the receptor or while signal transduction is occurring. For this reason, experimental results from accumulation assays are representative of overall effects that average the dynamic changes that occur to each ligand's structure as induced by light and are not fully macroscopically adjusted to a classical mixture of ligands with a particular stoichiometry.

Taken together, this study has highlighted that subtle changes in the interactions within the common $mGlu_5$ allosteric pocket can lead to substantial changes in an allosteric ligand's affinity, which have functional implications. This study also demonstrates that the reversible NAM activity of alloswitch-1 and MCS0331 translates *in vivo*. In a mouse model of inflammatory pain, which $mGlu_5$ NAMs have historically shown efficacy in[36], we show that intra-amygdala injection of either alloswitch-1 or MCS0331 rapidly and reversibly improves the mechanical pain threshold of mice to similar extents as that of the non-photoswitchable NAM, MPEP. Since previous and in-house studies have shown alloswitch-1 and MCS0331 to be selective NAMs for the $mGlu_5$, these data suggest that the ability of these ligands to exert negative cooperativity with the signaling efficacy of glutamate is essential to the ligands' *in vivo* efficacy.[12, 13] It is hypothesized that the key mechanism for their ability to reversible affect mechanical pain in mice, is due to their reduced affinity for the $mGlu_5$, following local *trans*-to-*cis* photoisomerization within the amygdala (both inside and outside the binding pocket), which leads to insufficient levels of receptor occupancy in order to have an analgesic effect, under 380 nm conditions. This effect can then be reversed by local 505 nm irradiation and *cis*-to-*trans* photoisomerization of ligands to their higher affinity (*trans*) states. We further predict that the change in affinity of these ligands is a result of a faster dissociation rate of the *cis*-forms of ligands from the receptor. We cannot though, discount the possibility that slower *cis*-isomer association rates may also impact the affinity and the prospect of ligands rebinding to $mGlu_5$ to then affect the biological outcomes of these compounds. These results add to a growing body of evidence for the practicality of using photoswitchable ligands to modulate GPCR activity in vivo and their potential advantages over more conventional pharmacological probes.[18, 21, 47-49] Given that the activity of photoswitchable ligands can be reversibly controlled in real-time under defined light conditions, the dynamic control of receptor activity in a site-specific manner is attainable with a rather good precision, in contrast to non-photoswitchable ligands.

In conclusion, this study has provided an in-depth pharmacological characterization of freely diffusible $mGlu_5$ photoswitchable allosteric modulators and we propose that the reversible NAM activity - both *in vitro* and *in vivo* - of alloswitch-1 and MCS0331 is a result of changes in affinity for their $mGlu_5$ binding site, under different light conditions. The data described here experimentally support the hypothesis that photoswitching between isomeric forms of these photoswitchable ligands is also possible within the binding pocket. This study will provide the framework for futures studies to investigate the mechanism of action of other photoswitchable ligands targeting different receptors and will help to understand GPCR molecular dynamics and function.

Methods

Materials

Sources of all materials are listed in supplementary information.

Photochemistry

Details of the photochemistry including absorption spectra, kinetics of *cis*-to-*trans* isomer relaxation, stability and reversibility and ^{1}H-NMR determination for alloswitch-1 and MCS0331 are listed in supplementary information.

Cell culture, transfections, inositol phosphate one (IP_1) accumulation assay and membrane preparations

Explanation of cell culture, transfections, the protocol for the inositol phosphate one (IP_1) accumulation assay and membrane preparations are listed in supplementary information.

MS Binding Assays

Equipment settings and compound synthesis are listed in the supporting information.

Alloswitch-1 and MCS0331 Saturation MS Binding Assays

$HmGlu_5$ membranes (20 μg/well) were incubated with test compounds (1 nM to 600 nM) for 1 h at 37°C, while shaking at 150 rpm, under dark, 500 nm or 380 nm conditions; final assay volume 300 μL/well. For all assays, black clear bottom 96-well plates (Greiner Bio-one) were placed over a 96-LED array plate (LEDA, Teleopto) connected to a LED array driver (LAD-1, Teleopto), for dark conditions half of each assay plate was covered with aluminum foil and light was pulsed underneath for 50/50 ms on/off at 0.12 mW/mm^2. The assay was stopped by rapid vacuum filtration through 1 μm GF filter multi-well plate (AcroPrep Advance 350 μL, Pall Corporation), pre-soaked for 1 h in 0.5% PEI, with an extraction plate manifold (Pall Corporation). Filter plates were washed 5 times with ice-cold binding buffer (150 μL) to remove unbound ligand and then dried for 1 h at 60ºC. Notably, the filtration and washing steps were performed under 380 nm illumination conditions. Samples were then washed 3 times with 100 μL of acetonitrile containing the corresponding IS to elute bound ligands and then once with ammonium bicarbonate buffer (10 mM, pH 7.5; 100 μL per well). Samples were transferred to HPLC vials and analyzed following the appropriate HPLC-MS/MS method (see “Chromatographic and mass spectrometric conditions” for more detail). Non-specific binding was determined in the presence of 10 μM VU0409106.

Alloswitch-1 and MCS0331 Dissociation MS Binding Assays

$HmGlu_5$ membranes (20 μg/well) were incubated with either 32 nM of alloswitch-1 or 15 nM of MCS0331, respectively, for 1 h at 37°C, while shaking at 150 rpm and in a final assay volume of 300 μL/well, under dark conditions. Following the association phase, the dissociation of ligands was initiated with 100 μM VU0409106 at

different time points (1 - 120 min), under dark or 380 nm conditions (50/50 ms off at 12V). Illumination of plates was performed as described in the previous section. The assay was stopped and samples were analyzed as described previously. Non-specific binding was determined in the presence of 10 μM VU0409106.

[^{3}H]-MPEP Equilibrium Binding

For [^{3}H]-MPEP competition binding assays, $hmGlu_5$ expressing membranes (10 μg/well) were incubated for 1 h at 37°C with ~ 10 nM [^{3}H]-MPEP and a range of concentrations of test compounds (100 pM to 10 μM), in the presence or absence of saturating concentrations of either 1 mM of glutamate or 30 μM of quisqualate [34, 35], under either dark, 500 nm or 380 nm illuminated conditions (final assay volume of 100 μL per well). For membranes that were incubated under light conditions, 96-well plates were paced over an LED plate (LEDA, Teleopto) and light was pulsed for 50/50 ms on/off at 12V. Binding assays were then terminated by rapid filtration through 1 μm GF multi-well plates (pre-soaked for 1 h in 0.5% PEI), and 4 washers with ice-cold binding buffer was used to separate bound and free radioligand. 100 μL of Ultima Gold™ was then added to each well and radioactivity was counted after at least 1 h of incubation on the MicroBeta plate counter (Perkin Elmer). MPEP (10 μM) was used to determine non-specific binding in all cases.

Animals

Experiments were performed on 8 to 12-week-old C57BL/6J males (Charles River). Animals were housed in groups of 3/cage, fed *ad libitum* and maintained under a 12 h light/dark cycle. Animals were treated in accordance with the European Community Council Directive 86/609. Experimental protocols were approved by the local authorities (regional animal welfare committee (CEEA-LR) with the guidelines of the French Agriculture and Forestry Ministry (C34-172-13). All efforts were made to minimize animal suffering and number.

Behavioral studies

Explanation of behavioral studies is listed in supplementary information.

Data analysis

For detailed explanation of curve fitting of datasets please refer to supplementary information.

Acknowledgments

We thank Carolina Cera and Teresa Sarrias (SimChem, IQAC-CSIC, Barcelona) and Anna Duran, Roser Borràs and Gloria Somalo (MCS group, IQAC-CSIC, Barcelona) for technical support. We thank Maria José Bleda Hernández (IQAC-CSIC, Barcelona) for statistical support. We thank Jean-Philippe Pin (IGF, Montpellier) for scientific support and contributions to this work. We thank Christine Enjalbal (IBMM, Montpellier), Thierry Durroux (IGF, Montpellier), Jean-Louis Banères (IBMM, Montpellier) and Guillaume Lebon (IGF, Montpellier) for scientific discussion. This research was supported by FEDER/Ministerio de Ciencia, Innovación y Universidades–Agencia

Estatal de Investigación (CTQ2017-89222-R and PCI2018-093047), the Catalan government (2017SGR1604), by CSIC (PICS program 08212), by Neuron-ERANET, by grants from the Agence Nationale de la Recherche (ANR-16-CE16-0010 and ANR-17-NEU3-0001 under the frame of Neuron Cofund) and by the Programme International de Collaboration Scientifique of the CNRS (PICS 08212). AEB was supported by the Labex EpiGenMed (program « Investissements d'avenir », ANR-10-LABX-12-01).

Author Contributions

M. R-O. and A.E.B. designed and performed *in vitro* photopharmacology assays, analyzed and discussed results, and wrote the paper, V. P. and A.E.B. performed photopharmacology *in vivo* assays, F.M. set-up *in vitro* photopharmacology assays, J.C.; J. F., X.G.S. synthesized compounds, X.G.S. also contributed to the writing of the paper, C.Z. set-up *in vivo* photopharmacology assays , L. M ., C. S., X.R. contributed to HPLC-MS binding assay development, X. R. also discussed results , C.G. and A.L. designed research, managed the project, revised results and wrote the paper.

This PDF is accompanied by supporting information, which includes:

Supplementary text, including materials and methods

Figures and legends S1 to S7

Tables and legends S1 to S4

SI References

References

1. Hauser, A. S., Attwood, M. M., Rask-Andersen, M., Schioth, H. B., and Gloriam, D. E. (2017) Trends in GPCR drug discovery: new agents, targets and indications, *Nature reviews. Drug discovery 16*, 829-842. *Drug discovery 16*, 829-842. DOI: 10.1038/nrd.2017.178.
2. Conn, P. J., and Pin, J. P. (1997) Pharmacology and functions of metabotropic glutamate receptors, *Annual review of pharmacology and toxicology 37*, 205-237. DOI: 10.1146/annurev.pharmtox.37.1.205.
3. Gregory, K. J., Noetzel, M. J., and Niswender, C. M. (2013) Pharmacology of metabotropic glutamate receptor allosteric modulators: structural basis and therapeutic potential for CNS disorders, *Progress in molecular biology and translational science 115*, 61-121. DOI: 10.1016/b978-0-12-394587-7.00002-6.
4. Pereira, V., and Goudet, C. (2018) Emerging Trends in Pain Modulation by Metabotropic Glutamate Receptors, *Frontiers in molecular neuroscience 11*, 464. DOI: 10.3389/fnmol.2018.00464.
5. Reiner, A., and Levitz, J. (2018) Glutamatergic Signaling in the Central Nervous System: Ionotropic and Metabotropic Receptors in Concert, *Neuron 98*, 1080-1098. DOI: 10.1016/j.neuron.2018.05.018.
6. Christopoulos, A., and Kenakin, T. (2002) G protein-coupled receptor allosterism and complexing, *Pharmacological reviews 54*, 323-374. DOI: 10.1124/pr.54.2.323.
7. Melancon, B. J., Hopkins, C. R., Wood, M. R., Emmitte, K. A., Niswender, C. M., Christopoulos, A., Conn, P. J., and Lindsley, C. W. (2012) Allosteric modulation of seven transmembrane spanning receptors: theory, practice, and opportunities for central nervous system drug discovery, *Journal of medicinal chemistry 55*, 1445-1464. DOI: 10.1021/jm201139r.
8. Walker, A. G., and Conn, P. J. (2015) Group I and group II metabotropic glutamate receptor allosteric modulators as novel potential antipsychotics, *Current opinion in pharmacology 20*, 40-45. DOI: 10.1016/j.coph.2014.11.003.
9. Christoffersen, G. R., Simonyi, A., Schachtman, T. R., Clausen, B., Clement, D., Bjerre, V. K., Mark, L. T., Reinholdt, M., Schmith-Rasmussen, K., and Zink, L. V. (2008) MGlu5 antagonism impairs exploration and memory of spatial and non-spatial stimuli in rats, *Behavioural brain research 191*, 235-245. DOI:10.1016/j.bbr.2008.03.032.

10. Rodriguez, A. L., Grier, M. D., Jones, C. K., Herman, E. J., Kane, A. S., Smith, R. L., Williams, R., Zhou, Y., Marlo, J. E., Days, E. L., Blatt, T. N., Jadhav, S., Menon, U. N., Vinson, P. N., Rook, J. M., Stauffer, S. R., Niswender, C. M., Lindsley, C. W., Weaver, C. D., and Conn, P. J. (2010) Discovery of novel allosteric modulators of metabotropic glutamate receptor subtype 5 reveals chemical and functional diversity and in vivo activity in rat behavioral models of anxiolytic and antipsychotic activity, *Molecular pharmacology 78*, 1105-1123. DOI: 10.1124/mol.110.067207.
11. Velema, W. A., Szymanski, W., and Feringa, B. L. (2014) Photopharmacology: beyond proof of principle, *Journal of the American Chemical Society 136*, 2178-2191. DOI: 10.1021/ja413063e.
12. Pittolo, S., Gomez-Santacana, X., Eckelt, K., Rovira, X., Dalton, J., Goudet, C., Pin, J. P., Llobet, A., Giraldo, J., Llebaria, A., and Gorostiza, P. (2014) An allosteric modulator to control endogenous G protein-coupled receptors with light, *10*, 813-815. DOI: 10.1038/nchembio.1612.
13. Gomez-Santacana, X., Pittolo, S., Rovira, X., Lopez, M., Zussy, C., Dalton, J. A., Faucherre, A., Jopling, C., Pin, J. P., Ciruela, F., Goudet, C., Giraldo, J., Gorostiza, P., and Llebaria, A. (2017) Illuminating Phenylazopyridines To Photoswitch Metabotropic Glutamate Receptors: From the Flask to the Animals, *ACS central science 3*, 81-91.
14. Font, J., Lopez-Cano, M., and Notartomaso, S. (2017) Optical control of pain in vivo with a photoactive mGlu5 receptor negative allosteric modulator, *6*. DOI: 10.7554/eLife.23545.
15. Agnetta, L., Kauk, M., Canizal, M. C. A., Messerer, R., and Holzgrabe, U. (2017) A Photoswitchable Dualsteric Ligand Controlling Receptor Efficacy, *56*, 7282-7287. DOI: 10.1002/anie.201701524.
16. Broichhagen, J., Johnston, N. R., von Ohlen, Y., Meyer-Berg, H., Jones, B. J., Bloom, S. R., Rutter, G. A., Trauner, D., and Hodson, D. J. (2016) Allosteric Optical Control of a Class B G-Protein-Coupled Receptor, *55*, 5865-5868. DOI: 10.1002/anie.201600957.
17. Broichhagen, J., Damijonaitis, A., Levitz, J., Sokol, K. R., Leippe, P., Konrad, D., Isacoff, E. Y., and Trauner, D. (2015) Orthogonal Optical Control of a G Protein-Coupled Receptor with a SNAP-Tethered Photochromic Ligand, *ACS central science 1*, 383-393. DOI: 10.1021/acscentsci.5b00260.
18. Hull, K., Morstein, J., and Trauner, D. (2018) In Vivo Photopharmacology, *118*, 10710-10747. DOI: 10.1021/acs.chemrev.8b00037.
19. Ricart-Ortega, M., Font, J., and Llebaria, A. (2019) GPCR photopharmacology, *Molecular and cellular endocrinology 488*, 36-51. DOI: 10.1016/j.mce.2019.03.003.
20. Berizzi, A. E., and Goudet, C. (2020) Strategies and considerations of G-protein-coupled receptor photopharmacology, *Advances in pharmacology 88*, 143-172. DOI: 10.1016/bs.apha.2019.12.001.
21. Zussy, C., Gomez-Santacana, X., Rovira, X., De Bundel, D., Ferrazzo, S., Bosch, D., Asede, D., Malhaire, F., Acher, F., Giraldo, J., Valjent, E., Ehrlich, I., Ferraguti, F., Pin, J. P., Llebaria, A., and Goudet, C. (2018) Dynamic modulation of inflammatory pain-related affective and sensory symptoms by optical control of amygdala metabotropic glutamate receptor 4, *Molecular psychiatry 23*, 509-520. DOI: 10.1038/mp.2016.223.
22. Rovira, X., Trapero, A., Pittolo, S., Zussy, C., Faucherre, A., Jopling, C., Giraldo, J., Pin, J. P., Gorostiza, P., Goudet, C., and Llebaria, A. (2016) OptoGluNAM4.1, a Photoswitchable Allosteric Antagonist for Real-Time Control of mGlu4 Receptor Activity, *Cell chemical biology 23*, 929-934. DOI: 10.1016/j.chembiol.2016.06.013.
23. Morstein, J., Hill, R. Z., Novak, A. J. E., Feng, S., Norman, D. D., Donthamsetti, P. C., Frank, J. A., Harayama, T., Williams, B. M., Parrill, A. L., Tigyi, G. J., Riezman, H., Isacoff, E. Y., Bautista, D. M., and Trauner, D. (2019) Optical control of sphingosine-1-phosphate formation and function, *15*, 623-631. DOI: 10.1038/s41589-019-0269-7.
24. Agnetta, L., Bermudez, M., Riefolo, F., Matera, C., Claro, E., Messerer, R., Littmann, T., Wolber, G., Holzgrabe, U., and Decker, M. (2019) Fluorination of Photoswitchable Muscarinic Agonists Tunes Receptor Pharmacology and Photochromic Properties, *J Med Chem 62*, 3009-3020. DOI: 10.1021/acs.jmedchem.8b01822.
25. Bahamonde, M. I., Taura, J., Paoletta, S., Gakh, A. A., Chakraborty, S., Hernando, J., Fernandez-Duenas, V., Jacobson, K. A., Gorostiza, P., and Ciruela, F. (2014) Photomodulation of G protein-coupled adenosine receptors by a novel light-switchable ligand, *Bioconjug Chem 25*, 1847-1854. DOI: 10.1021/bc5003373.
26. Hauwert, N. J., Mocking, T. A. M., Da Costa Pereira, D., Lion, K., Huppelschoten, Y., Vischer, H. F., De Esch, I. J. P., Wijtmans, M., and Leurs, R. (2019) A Photoswitchable Agonist for the Histamine H3 Receptor, a Prototypic Family A G-Protein-Coupled Receptor, *58*, 4531-4535. DOI: 10.1002/anie.201813110.
27. Schonberger, M., and Trauner, D. (2014) A photochromic agonist for mu-opioid receptors, *Angewandte Chemie (International ed. in English) 53*, 3264-3267. DOI: 10.1002/anie.201309633.
28. Jones, B. J., Scopelliti, R., Tomas, A., Bloom, S. R., Hodson, D. J., and Broichhagen, J. (2017) Potent Prearranged Positive Allosteric Modulators of the Glucagon-like Peptide-1 Receptor, *6*, 501-505. DOI: 10.1002/open.201700062.
29. Christopoulos, A. (2014) Advances in G protein-coupled receptor allostery: from function to structure, *Molecular pharmacology 86*, 463-478. DOI: 10.1124/mol.114.094342.
30. Dalton, J. A., Lans, I., Rovira, X., Malhaire, F., Gomez-Santacana, X., Pittolo, S., Gorostiza, P., Llebaria, A., Goudet, C., Pin, J. P., and Giraldo, J. (2016) Shining Light on an mGlu5 Photoswitchable NAM: A Theoretical Perspective, *Current neuropharmacology 14*, 441-454. DOI: 10.2174/1570159x13666150407231417.
31. Leach, K., Sexton, P. M., and Christopoulos, A. (2007) Allosteric GPCR modulators: taking advantage of permissive receptor pharmacology, *Trends in pharmacological sciences 28*, 382-389. DOI: 10.1016/j.tips.2007.06.004.
32. Black, J. W., and Leff, P. (1983) Operational models of pharmacological agonism, *Proceedings of the Royal Society of London. Series B, Biological sciences 220*, 141-162. DOI: 10.1098/rspb.1983.0093.

33. Berizzi, A. E., Gentry, P. R., Rueda, P., Den Hoedt, S., Sexton, P. M., Langmead, C. J., and Christopoulos, A. (2016) Molecular Mechanisms of Action of M5 Muscarinic Acetylcholine Receptor Allosteric Modulators, *Molecular pharmacology 90*, 427-436. DOI: 10.1124/mol.116.104182.
34. Bradley, S. J., Langmead, C. J., Watson, J. M., and Challiss, R. A. (2011) Quantitative analysis reveals multiple mechanisms of allosteric modulation of the mGlu5 receptor in rat astroglia, *Molecular pharmacology 79*, 874-885. DOI: 10.1124/mol.110.068882.
35. Gregory, K. J., Noetzel, M. J., Rook, J. M., Vinson, P. N., Stauffer, S. R., Rodriguez, A. L., Emmitte, K. A., Zhou, Y., Chun, A. C., Felts, A. S., Chauder, B. A., Lindsley, C. W., Niswender, C. M., and Conn, P. J. (2012) Investigating metabotropic glutamate receptor 5 allosteric modulator cooperativity, affinity, and agonism: enriching structure-function studies and structure-activity relationships, *Molecular pharmacology 82*, 860-875. DOI: 10.1124/mol.112.080531.
36. Kolber, B. J., Montana, M. C., Carrasquillo, Y., Xu, J., Heinemann, S. F., Muglia, L. J., and Gereau, R. W. t. (2010) Activation of metabotropic glutamate receptor 5 in the amygdala modulates pain-like behavior, *The Journal of neuroscience : the official journal of the Society for Neuroscience 30*, 8203-8213. DOI: 10.1523/jneurosci.1216-10.2010.
37. Sykes, D. A., Moore, H., Stott, L., Holliday, N., Javitch, J. A., Lane, J. R., and Charlton, S. J. (2017) Extrapyramidal side effects of antipsychotics are linked to their association kinetics at dopamine D(2) receptors, *Nature communications 8*, 763. DOI: 10.1038/s41467-017-00716-z.
38. Klein Herenbrink, C., Sykes, D. A., Donthamsetti, P., Canals, M., Coudrat, T., Shonberg, J., Scammells, P. J., Capuano, B., Sexton, P. M., Charlton, S. J., Javitch, J. A., Christopoulos, A., and Lane, J. R. (2016) The role of kinetic context in apparent biased agonism at GPCRs, *Nature communications 7*, 10842. DOI: 10.1038/ncomms10842.
39. Litschig, S., Gasparini, F., Rueegg, D., Stoehr, N., Flor, P. J., Vranesic, I., Prezeau, L., Pin, J. P., Thomsen, C., and Kuhn, R. (1999) CPCCOEt, a noncompetitive metabotropic glutamate receptor 1 antagonist, inhibits receptor signaling without affecting glutamate binding, *Molecular pharmacology 55*, 453-461. PubMed:10051528.
40. Dore, A. S., Okrasa, K., Patel, J. C., Serrano-Vega, M., Bennett, K., Cooke, R. M., Errey, J. C., Jazayeri, A., Khan, S., Tehan, B., Weir, M., Wiggin, G. R., and Marshall, F. H. (2014) Structure of class C GPCR metabotropic glutamate receptor 5 transmembrane domain, *Nature 511*, 557-562. DOI: 10.1038/nature13396.
41. Christopher, J. A., Aves, S. J., Bennett, K. A., Dore, A. S., Errey, J. C., Jazayeri, A., Marshall, F. H., Okrasa, K., Serrano-Vega, M. J., Tehan, B. G., Wiggin, G. R., and Congreve, M. (2015) Fragment and Structure-Based Drug Discovery for a Class C GPCR: Discovery of the mGlu5 Negative Allosteric Modulator HTL14242 (3-Chloro-5-[6-(5-fluoropyridin-2-yl)pyrimidin-4-yl]benzonitrile), *Journal of medicinal chemistry 58*, 6653-6664. DOI: 10.1021/acs.jmedchem.5b00892.
42. Wood, M. R., Hopkins, C. R., Brogan, J. T., Conn, P. J., and Lindsley, C. W. (2011) "Molecular switches" on mGluR allosteric ligands that modulate modes of pharmacology, *Biochemistry 50*, 2403-2410. DOI: 10.1021/bi200129s.
43. O'Brien, J. A., Lemaire, W., Chen, T. B., Chang, R. S., Jacobson, M. A., Ha, S. N., Lindsley, C. W., Schaffhauser, H. J., Sur, C., Pettibone, D. J., Conn, P. J., and Williams, D. L., Jr. (2003) A family of highly selective allosteric modulators of the metabotropic glutamate receptor subtype 5, *Molecular pharmacology 64*, 731-740. DOI: 10.1124/mol.64.3.731.
44. Gregory, K. J., Nguyen, E. D., Reiff, S. D., Squire, E. F., Stauffer, S. R., Lindsley, C. W., Meiler, J., and Conn, P. J. (2013) Probing the metabotropic glutamate receptor 5 (mGlu(5)) positive allosteric modulator (PAM) binding pocket: discovery of point mutations that engender a "molecular switch" in PAM pharmacology, *Molecular pharmacology 83*, 991-1006. DOI: 10.1124/mol.112.083949.
45. Gómez-Santacana, X., Rovira, X., Dalton, J. A., Goudet, C., Pin, J. P., Gorostiza, P., Giraldo, J., and Llebaria, A. (2014) A double effect molecular switch leads to a novel potent negative allosteric modulator of metabotropic glutamate receptor 5, *MedChemComm 5*, 1548-1554. DOI: 10.1039/C4MD00208C.
46. Perez-Benito, L., Doornbos, M. L. J., Cordomi, A., Peeters, L., Lavreysen, H., Pardo, L., and Tresadern, G. (2017) Molecular Switches of Allosteric Modulation of the Metabotropic Glutamate 2 Receptor, *Structure (London, England : 1993) 25*, 1153-1162.e1154. DOI: 10.1016/j.str.2017.05.021.
47. Acosta-Ruiz, A., Gutzeit, V. A., Skelly, M. J., Meadows, S., Lee, J., Parekh, P., Orr, A. G., Liston, C., Pleil, K. E., Broichhagen, J., and Levitz, J. (2020) Branched Photoswitchable Tethered Ligands Enable Ultra-efficient Optical Control and Detection of G Protein-Coupled Receptors In Vivo, *Neuron 105*, 446-463 e413. DOI: 10.1016/j.neuron.2019.10.036.
48. Donthamsetti, P. C., Broichhagen, J., Vyklicky, V., Stanley, C., Fu, Z., Visel, M., Levitz, J. L., Javitch, J. A., Trauner, D., and Isacoff, E. Y. (2019) Genetically Targeted Optical Control of an Endogenous G Protein-Coupled Receptor, *Journal of the American Chemical Society 141*, 11522-11530. DOI: 10.1021/jacs.9b02895.
49. Frank, J. A., Yushchenko, D. A., Fine, N. H. F., Duca, M., Citir, M., Broichhagen, J., Hodson, D. J., Schultz, C., and Trauner, D. (2017) Optical control of GPR40 signalling in pancreatic beta-cells, *Chem Sci 8*, 7604-7610. DOI: 10.1039/c7sc01475a.

For Table of Contents Use Only

Mechanistic insights into light-driven allosteric control of GPCR biological activity

Maria Ricart-Ortega[a,c,1], Alice E. Berizzi[c,1], Vanessa Pereira[c], Fanny Malhaire[c], Juanlo Catena[a], Joan Font[c], Xavier Gómez-Santacana[c], Lourdes Muñoz[a,b], Charleine Zussy[c], Carmen Serra[a,b], Xavier Rovira[a], Cyril Goudet[c,*] and Amadeu Llebaria[a,b,*]

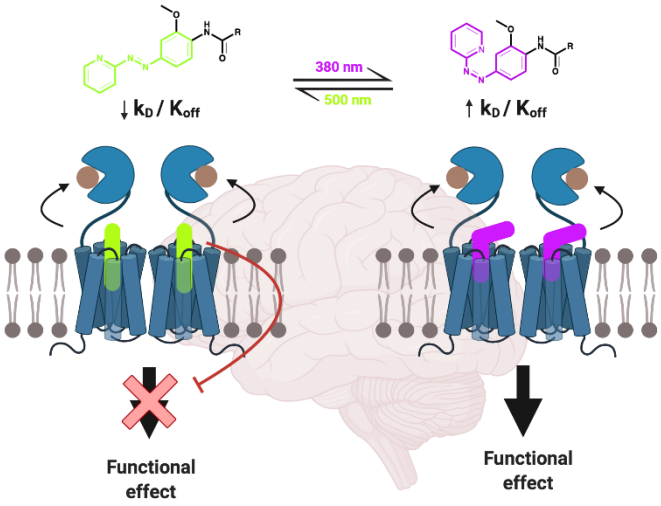

Alloswitch-1 and MCS0331, two photoswitchable negative allosteric modulators, have higher affinity for the $mGlu_5$ allosteric pocket in their stable *trans*-configuration, under dark or 500 nm conditions. During 380 nm conditions, *trans*-to-*cis* azobenzene photoisomerization occurs inside and outside the binding pocket. The resulting ligand *cis*-isomers have reduced affinity and dissociate faster from the receptor. Differences in affinity and binding kinetics for each ligand configuration , in part, explain the *in vitro* and *in vivo* pharmacological behavior of these freely diffusible photoswitchable ligands under changing light conditions.

ACS Pharmacology and Translational Science

Supporting Information for

Mechanistic insights into light-driven allosteric control of GPCR biological activity

Maria Ricart-Ortega[a,c,1], Alice E. Berizzi[c,1], Vanessa Pereira[c], Fanny Malhaire[c], Juanlo Catena[a], Joan Font[c], Xavier Gómez-Santacana[c], Lourdes Muñoz[a,b], Charleine Zussy[c], Carmen Serra[a,b], Xavier Rovira[a], Cyril Goudet[c,*] and Amadeu Llebaria[a,b,*]

[a]MCS, Laboratory of Medicinal Chemistry & Synthesis, Department of Biological Chemistry, Institute for Advanced Chemistry of Catalonia (IQAC-CSIC), Barcelona, Spain; [b]SIMchem, Service of Synthesis of High Added Value Molecules, Institute for Advanced Chemistry of Catalonia (IQAC-CSIC), Barcelona, Spain; [c]IGF, University of Montpellier, CNRS, INSERM, F-34094 Montpellier, France.

[1] equally contributed to this work

* Amadeu Llebaria (ORCID: 0000-0002-8200-4827) and Cyril Goudet (ORCID: 0000-0002-8255-3535)

Email: amadeu.llebaria@iqac.csic.es and cyril.goudet@igf.cnrs.fr

This PDF file includes:

Methods

Materials

HEK 293 cells were obtained from ATCC® CRL-1573™ (Molsheim, France). The $hmGlu_5$ construct was prepared in-house, while the mouse $mGlu_5$ construct was purchased from GeneCust (Boynes, France). Dulbecco's modified Eagle medium (DMEM), glutamate-free DMEM GlutaMAX-I, enzyme-free cell dissociation buffer and fetal bovine serum were purchased from Thermo Fisher Scientific. Antibiotics, Polyethylenimine (PEI) and L-glutamic acid were purchased from Sigma-Aldrich. [^{3}H]-MPEP was purchased from American Radiolabelled Chemicals, Inc (ARC; St Louis, USA). Ultima Gold™ was purchased from PerkinElmer. The IP_1 assay kit was a generous gift from Cisbio bioassays (Codolet, France). Quisqualate and VU0409106 were obtained from Tocris Biosciences (Bristol, United Kingdom). Alloswitch-1, MCS0331 and internal standard (IS) compounds (MCS0397 and MCS0394, synthesis procedures detailed below), were synthesized in MCS laboratory (Barcelona, Spain). All the chemicals and solvents were purchased from commercial suppliers and used without purification, except the anhydrous solvents, including dimethylformamide (DMF), which were treated previously through a system of solvent purification (PureSolv), degasified with inert gases and dried over alumina or molecular sieves. Acetonitrile and methanol (HPLC grade) were purchased from Thermo Fisher Scientific (Nimes, France). All other reagents and chemicals were purchased from Sigma-Aldrich (Saint-Quentin-Falavier, France).

Methods

Photochemistry

UV-Vis spectra of alloswitch-1 and MCS0331 were obtained using a SPARK 20M Multimode Microplate Reader (Tecan). The photoswitchable compounds (5 or 30 μM) were diluted in 3 or 5% DMSO MS binding buffer (25 mM HEPES, 100 mM NaCl and 2.5 mM $MgCl_2$, pH 7.5) and photochemistry assays were performed in a transparent 96-well plate (Deltalab) under either dark or light conditions (3 min of continuous illumination with a 96-LED array plate (LEDA, Teleopto) connected to a LED array driver (LAD-1, Teleopto)). Irradiance (light power/surface unit) was set to 0.09 mW/mm^2 for the wavelength 365 nm, 0.09 mW/mm^2 for 380 nm, 0.19 mW/mm^2 for 405 nm, 0.13 mW/mm^2 for 420 nm, 0.17 mW/mm^2 for 455 nm, 0.14 mW/mm^2 for 470 nm, 0.10 mW/mm^2 for 500 nm, 0.09 mW/mm^2 for 530 nm, and 0.14 mW/mm^2 for 550 nm. Irradiance values were measured using a Thorlabs PM100D power energy meter connected to a standard photodiode power sensor (S120VC).

Absorption spectra

UV-Vis absorption spectra of alloswitch-1 and MCS0331 were obtained by scanning wavelengths between 300 nm - 600 nm, in 2 nm increments. UV-Vis spectra report values for dark and light conditions for wavelengths 365 nm, 380 nm, 405 nm, 420 nm, 455 nm, 470 nm, 500 nm, 530 nm and 550 nm.

Kinetics of *cis*-to-*trans* isomer relaxation

The *cis*-to-*trans* thermal relaxation curves for alloswitch-1 and MCS0331 were obtained by measuring the UV-Vis absorbance of the azo compounds at a single wavelength (376 nm) after being illuminated with 380 nm light. The UV-Vis absorbances were recorded every 30 s by prolonged absorbance measuring, at 37ºC, in the dark.

Stability and reversibility

Repeated *trans*-to-*cis* isomerization cycles of alloswitch-1 and MCS0331 were recorded under either dark, 500 nm or 380 nm conditions by measuring absorbance at determined single wavelength (376 nm).

^{1}H-NMR determination

^{1}H-NMR spectra of alloswitch-1 and MCS0331 were acquired using a Brucker Avance-III 500 MHz spectrometer equipped with a z-axis pulsed field gradient triple resonance (^{1}H, ^{13}C, ^{15}N) TCI cryoprobe. Isomerization of 1 mM

alloswitch-1 in DMSO-*d6* and 500 μM MCS0331 5% DMSO-*d6* in D_2O was analyzed under either dark or 380 nm conditions (3 min of continuous illumination with a 96-LED array plate (LEDA, Teleopto) connected to a LED array driver (LAD-1, Teleopto)) at 25ºC and 12ºC, respectively. Irradiance was set to 0.09 mW/mm^2 for the wavelengths 380 nm and 0.10 mW/mm^2 for 500 nm. The illumination was performed in a Wilmad screw-cap NMR tube with 700 μl final volume. Acquisitions consisted in 8 scans using the zg pulse sequence and every sample was locked, tuned and shimmed before new experiment acquisition.

Cell culture and Transfections

HEK 293 cells were cultured in DMEM supplemented with 10 % FBS and were maintained at 37°C in a humidified atmosphere with 5 % CO_2. Cells were transfected with either the human or mouse $mGlu_5$ by electroporation as previously described[1], with the exception that 8 μg of protein of the mouse $mGlu_5$ was used to transfect 10 million cells. For the transient transfection of the $mGlu_5$ in HEK 293 cells; ambient glutamate was maintained at minimal concentrations by co-transfection with the excitatory amino acid transporter 1 (EAAC1). The $hmGlu_5$ construct contained a Flag and SNAP tag and was prepared as previously described in[2], while the mouse mGlu5 construct contained a HA tag in the *N* terminus, respectively, to enable cell surface expression measurement. HEK 293 cells stably expressing the $hmGlu_5$ were maintained in the presence of 15 μg/mL blasticidin and 100 μg/mL of Hygromycine B at 37°C in a humidified atmosphere with 5 % CO_2. All cells were sub-cultured every two to three days in a 1:3 ratio after reaching 80 % confluency with 5 mL of trypsin to detach cells, and incubated in a humidified atmosphere at 37°C, 5% CO_2 for 2 - 5 min.

Inositol phosphate one (IP_1) accumulation

The IP_1 assay kit (Cisbio Bioassays, France) was used for the direct quantitative measurement of myoinositol 1-phosphate in HEK 293 cells transiently transfected with the human or mouse $mGlu_5$ and EAAC1 as described previously[3], with the exception that cells were seeded overnight at 100,000 per well into black, clear-bottom 96-well culture plates (Greiner Bio-one). Cells were stimulated with various concentrations of orthosteric and/or allosteric compounds, and were then incubated for 30 min at 37°C, 5% CO_2 in either dark or light conditions. Responses were normalized to that of a single, maximal concentration of quisqualate (10 μM). When illuminated, culture plates were placed above a 96-LED array plate (LEDA, Teleopto) connected to a LED array driver (LAD-1, Teleopto) with light pulsed for 50/50 ms on/off rather than continuous illumination to avoid overheating the cells and compromising the integrity of the assay. Irradiance was set to 0.09 mW/mm^2 for illumination at 365 nm, 0.12 mW/mm^2 at 380 nm, 0.20 mW/mm^2 at 405 nm, 0.10 mW/mm^2 at 420 nm, 0.10 mW/mm^2 at 455 nm, 0.15 mW/mm^2 at 470 nm, 0.13 mW/mm^2 at 500 nm, and 0.05 mW/mm^2 at 530 nm, with the exception of experiments where fine-tuning of irradiance for the 380 nm light were performed. For these experiments, irradiance varies from 0.02 - 0.15 mW/mm^2.

To determine functional affinity estimates of the orthosteric agonists used in these studies additional IP_1 assays were performed as described previously, but on cells that were transiently transfected with a range of concentrations of $hmGlu_5$ DNA (0.1 μg to 1 μg per 10 million cells).

Membrane preparation for MS binding and [^{3}H]-MPEP binding assays

Membranes were prepared from HEK 293 cells stably expressing the $hmGlu_5$ as follows. Cells were grown in 150 mm culture dishes and were harvested 24 h after induction with 1 μg/mL doxycycline (Sigma-Aldrich). Cells were centrifuged at 300 g for 5 min and then resuspended in 5 mL ice-cold homogenisation buffer (25 mM HEPES, 10 mM EDTA, 2.5 mM $MgCl_2$; pH 7.5). Cell suspensions were homogenised with 3 x 20 s bursts with an ultrasonic cell disruptor (SFX 150, Branson), which were separated by 20 s periods on ice. Cell homogenates were then

centrifuged at 600 g for 10 min at 4°C. The supernatant was collected and transferred to a centrifuge tube, the remaining cell pellet was re-suspended in homogenisation buffer, re-homogenised and centrifuged as previous. The supernatant was pooled and centrifuged at high speed (40 000 g, 60 min, 4°C). The final pellet was re-suspended in MS binding storage buffer (25 mM HEPES, 1 mM EDTA and 2.5 mM $MgCl_2$, pH 7.5) or [^{3}H]-MPEP binding buffer (110 mM NaCl, 5.4 mM KCl, 1.8 mM $CaCl_2$, 1 mM $MgSO_4$, 25 mM glucose, 50 mM HEPES, 58 mM sucrose; pH 7.4) to give a final protein concentration of ~1.5 to 2.5 mg/mL and then was stored at -80°C. Protein concentrations were determined by BCA protein assay kit as per the instructions of the supplier.

MS Binding Assays

Synthesis of internal standard (IS) compounds

Equipment settings

Reactions were monitored by thin layer chromatography (60 F, 0.2 mm, Macherey-Nagel) by visualization under 254 and/or 365 nm lamp. Purification was made by flash column chromatography using Panreac silica gel 60, 40-63 microns RE or by Isolera-Biotage equipment (SNAP KP-C18-HS-12g column; A: 0.05 % formic acid in water and B: 0.05 % formic acid in acetonitrile; 5 % B 3 column volume (CV), 5 % B - 100 % B 18 CV, 100 % B 5 CV). Nuclear magnetic resonance (NMR) spectrometry was performed using a Varian Mercury 400 MHz. Chemical shifts δ are reported in parts per million (ppm) against the reference compound (Chloroform δ = 7.26 ppm (^{1}H), δ = 77.16 ppm (^{13}C), and DMSOδ_6 δ = 2.50ppm (^{1}H), δ = 39.52 ppm (^{13}C). High Performance Liquid Chromatography (HPLC) analysis was performed on a 2795 Alliance HPLC system (Waters) equipped with an 1100 diode array detector (Agilent). Chromatographic separations were performed with a Zorbax Extend C18 column (2.1 x 50 mm, 3.5 μm, Agilent) with a Zorbax Extend C18 pre-column (2.1 x 12.5 mm, 5 μm, Agilent). The mobile phase used was a mixture of solvent A (0.05 % formic acid in water) and solvent B (0.05 % formic acid in acetonitrile) with a flow rate of 0.5 mL/min. The initial mobile phase composition was 5 % solvent B, held for 0.5 min. Then, changed to 100 % (over 5 min) and held at these conditions for 2 min before returning to the initial conditions. For all experiments, 10 μL of sample diluted in acetonitrile was injected. Mass spectrometry (MS) detection was carried out on a Quattro micro triple quadrupole mass spectrometer (Waters), using ESI source in positive ion mode. Melting points were measured with Melting Point B-545 (Büchi), ramp 0.5 ºC/min with a digital temperature measurement.

Synthesis of MCS0397 (deuterated alloswitch-1)

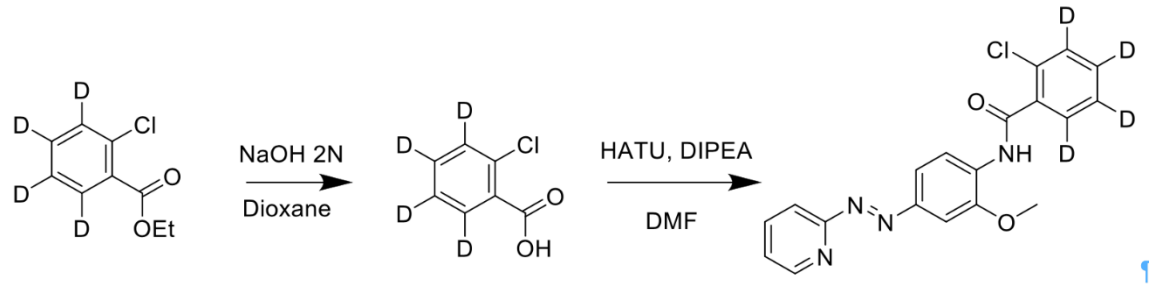

A **B** **C**

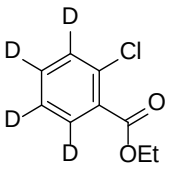

Ethyl 2-chlorobenzoate-3,4,5,6-*d*$_4$ (A). The synthesis of ethyl 2-chlorobenzoate-3,4,5,6-*d*$_4$ (A), was previously described in the literature.[4]

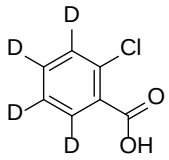

2-Chlorobenzoic acid 3,4,5,6-*d*$_4$ (B). NaOH 2 N (5.63 mL, 11.26 mmol) was added to a solution of ethyl 2-chlorobenzoate-3,4,5,6-*d*$_4$ (A) (0.425 g, 2.253 mmol) in dioxane (5.63 mL), under ice-cooled stirring. The reaction mixture was left at room temperature for 12 h and then quenched with 1M HCl (until pH = 1). After that, the mixture was concentrated to remove the dioxane and ethyl alcohol. The white precipitate formed was filtered. After drying, the compound B was obtained (149 mg, 41 % yield) as a white solid. HPLC/DAD: purity (abs = 254 nm) = 100 %; RT = 2.79 min, m/z: 161 $[M+1]^+$.

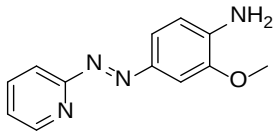

2-Methoxy-4-(pyridin-2-yldiazenyl)aniline (D). The synthesis of 2-methoxy-4-(pyridin-2-yldiazenyl)aniline (D), was as previously described in the literature.[5]

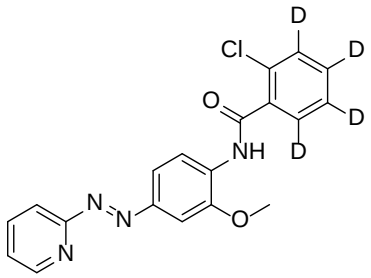

(2-Chloro-N-(2-methoxy-4-(pyridin-2-yldiazenyl)phenyl)benz-3,4,5,6-*d*$_4$-amide (C). To a stirred dispersion of 2-clorobenzoic acid 3,4,5,6-*d*$_4$ (B) (63 mg, 0.39 mmol) and HATU (149 mg, 0.39 mmol) in DMF (2 mL); *N*-ethyl-*N*-isopropylpropan-2-amine (100 µl, 0.59 mmol) followed by 2-methoxy-4-(pyridin-2-yldiazenyl)aniline (D) (90 mg, 0.39 mmol) were added. The reaction mixture was stirred at room temperature for 6 days. The reaction was diluted with water and extracted with EtOAc and the organic layer was washed with water (x3) and brine solution (x3), dried over anhydrous Na_2SO_4, filtered and evaporated. The residue was purified by reversed-phase flash chromatography, by using an Isolera - Biotage, yielding 27 mg (18 %) of an orange-red compound identified as compound C. ^{1}H NMR (400 MHz, $CDCl_3$) δ 8.82 (br, 1H), 8.78 (d, *J* = 8.4 Hz, 1H), 8.73 (dt, 1H, *J* = 4.8, 2 Hz, 1H), 7.90 (m, 1H), 7.86-7.81 (m, 2H), 7.65 (d, *J* = 2.0 Hz, 1H), 7.39 (dddd, *J* =7.3, 4,8, 1.2, 0,8 Hz, 1H), 3.97 (s, 3H). ^{13}C NMR (101 MHz, $CDCl_3$) δ 164.31, 163.04, 149.46, 148.71, 148.64, 138.30, 134.88, 131.55, 130.69, 130.40, 130.14, 129.87, 129.87, 124.98, 123.05, 119.26, 114.49, 100.54, 56.22. HRMS (m/z): $[M+H]^+$ calculated for $C_{19}H_{12}D_4ClN_4O_2$, 371.1213; found, 371.1206. HPLC/DAD: purity (abs = 254 nm) = 100 %; RT = 3.78 min. m.p. 153.7-154.5 ºC.

Synthesis of MCS0394 (deuterated MCS0331)

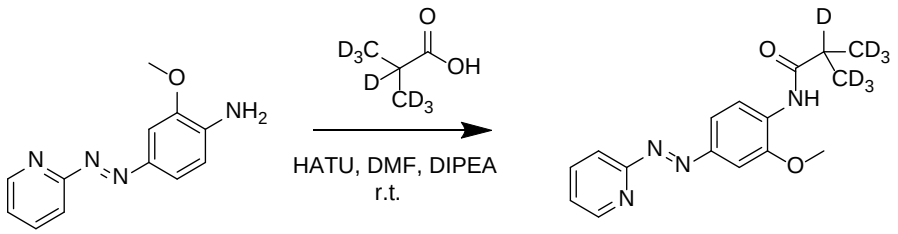

D **E**

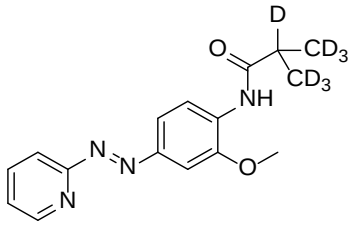

***N*-(2-Methoxy-4-(pyridin-2-yldiazenyl)phenyl)isobutyrnamide-d_7 (E).** A dispersion of isobutyric acid-d_7 (56 mg, 0.59 mmol), HATU (224 mg, 0.59 mmol), *N*-ethyl-*N*-isopropylpropan-2-amine (150 µl, 0.88mmol) and 2-methoxy-4-(pyridin-2-yldiazenyl)aniline (D) (134 mg, 0.59 mmol) in DMF (3 mL) was stirred at room temperature for 72 h. Then, the reaction was diluted with water and extracted with EtOAc, the organic layer was washed with water (x3) and brine solution (x3), dried over anhydrous Na_2SO_4, filtered and evaporated. The residue was purified by reverse-phase flash chromatography, by using Isolera-*Biotage* equipment, yielding 42 mg (23 %) of a red compound identified as compound F.^{1}H NMR (400 MHz, $CDCl_3$) δ 8.73 – 8.68 (m, 1H), 8.61 (d, *J* = 8.5 Hz, 1H), 8.01 (s, 1H), 7.87 (ddd, *J* = 8.1, 7.3, 1.9 Hz, 1H), 7.79 (dt, *J* = 8.1, 1.1 Hz, 1H), 7.75 (dd, *J* = 8.6, 2.1 Hz, 1H), 7.58 (d, *J* = 2.1 Hz, 1H), 7.37 (ddd, *J* = 7.3, 4.8, 1.2 Hz, 1H), 3.95 (s, 3H).^{13}C NMR (101 MHz, $CDCl_3$) δ 164.68, 162.92, 149.23, 148.26, 148.11, 138.47, 132.01, 124.96, 123.26, 118.79, 114.34, 100.22, 56.09 (quaternary deuterated carbons were not detected). HRMS (m/z): $[M+H]^+$ calculated for $C_{16}H_{12}D_7N_4O_2$, 306.1947; found, 306.1937. HPLC/DAD: purity (abs = 254 nm) = 95.1 %; RT = 3.39 min. m.p. 45.9-47.2ºC.

Synthesis of MCS0455 (deuterated MPEP)

Synthesis procedures were described in[2].

Chromatographic and mass spectrometric conditions

Chromatographic separations were performed with a Zorbax Extend C18 column (2.1 x 50 mm, 3.5 µm, Agilent) with a Zorbax Extend C18 pre-column (2.1 x 12.5 mm, 5 µm, Agilent), HPLC analysis was performed on a Thermo Scientific Dionex UltiMate 3000 High-Performance Liquid Chromatography system equipped with a pump (LPG-3400SD), and an auto-sampler (ACC-3000T) fitted with a thermostated column compartment. Gradient HPLC method was used for the analysis of alloswitch-1, MCS0331, VU0409106 and IS compounds (MCS0397 and MCS0394, respectively). The mobile phase consisted of solvent A (10 mM ammonium bicarbonate pH 7) and solvent B (acetonitrile) with a flow rate of 0.9 mL/min. The initial mobile phase composition for mixture 1 (alloswitch-1, MCS0397 and VU0409106) was 5 % solvent B, changed to 60 % (for 1 min) and then to 100 % (for 1 min). Then it was held for 3 min under these conditions, before returning to the initial conditions within 1 min. These conditions were maintained for 2 min to allow the column to equilibrate. In contrast, the initial mobile phase composition for mixture 2 (MCS0331, MCS0394 and VU0409106) was 5 % solvent B, changed to 100 % (for 3 min) and was then maintained under these conditions for 3 min, followed by the return to the initial conditions within 1 min. These

conditions were maintained for 3 min for column equilibration. For all experiments, the column and sampler temperature was set to 40 ºC and 10 ºC, respectively. The injection volume was 100 μL for alloswitch-1 and 10 μL for MCS0331 HPLC methods, respectively.

Mass spectrometry detection was carried out on a LTQ XL ion trap mass spectrometer (Thermo Scientific), using ESI source in positive ion mode. Quantification was performed using single reaction monitoring (SRM) mode with the transition of m/z 367.1 → 213 ± 2, 260 ± 2, 334 ± 2 for alloswitch-1, m/z 371.1 → 213 ± 2, 264 ± 2, 338 ± 2 for MCS0397, 299.0 → 229 ± 2 for MCS0331, m/z 306.0 → 230 ± 2 for MCS0394 and m/z 331.1 → 217 ± 2, 313 ± 2 for VU0409106. The optimal source parameters for mixture 1 were as follows: sheath gas flow at 60, aux gas flow at 10, sweep gas flow at 10, capillary temperature at 300 ºC, source voltage at 3.5 kV, capillary voltage at 10 V and tube lens at 85 V. The preferred source parameters for mixture 2 were as follows: sheath gas flow was at 60, aux gas flow at 10, sweep gas flow at 10, capillary temperature at 300 ºC, source voltage at 3 kV, capillary voltage at 0 V and tube lens at 75 V. The compound dependent parameter normalized collision energy (CE) was set at 40 % for alloswitch-1 and MCS0397, 25 % for MCS0331, 25 % for MCS0394 and 25 % for VU0409106. The compound dependent parameter normalized Act Q was set to 0.4 % for alloswitch-1 and MCS0397, and 0.25 % for MCS0331, MCS0394 and VU0409106. The compound dependent parameter Act Time was set to 40 ms for alloswitch-1 and MCS0397, 60 ms for MCS0331 and MCS0394 and 30 ms for VU0409106. The wideband activation option was selected for both mixtures. System control was performed by Thermo Xcalibur 2.2 software (Thermo Scientific). Chromatographic and mass spectrometric conditions for MPEP, MCS0455 and VU0409106 were detailed in[2].

Preparation of calibration curves and quality control samples

Calibration curves were prepared for mixture 1 (alloswitch-1, MCS0397 and VU0409106) and mixture 2 (MCS0331, MCS0394 and VU0409106) as previously described in[2], with the exception that the calibration curve for mixture 2 with final concentrations of 0.5 - 50 nM was obtained from working solutions (10 - 200 nM).

Quality control (QC) samples of mixture 1 with final concentrations of 0.125 nM (Lower limit of quantification; LLOQ), 0.35 nM (Lower; L), 10 nM (Medium; M), 20 nM (Higher; H) and 25 nM (Upper limit of quantification; ULOQ) were prepared as reported in[2]. While, QC samples of mixture 2 were 0.5 nM (LLOQ), 1.25 nM (L), 20 nM (M), 37.5 nM (H) and 50 nM (ULOQ) and were obtained in the same way as previously explained.
Preparation of MPEP, MCS0455 and VU0409106 calibration curves and quality control samples were explained in[2].

Analytical method validation

A full validation process was conducted in order to comply with *the guidance of industry bioanalytical method validation* as recommended by the FDA.[6] Selectivity, carry over, linearity, within-run and between-runs accuracy and precision, matrix factor and extraction recovery for each analyte and the IS compounds were carried out as previously detailed in[2] and satisfied the indicated criteria. The LLOQ was confirmed to be 0.125 nM for alloswitch-1 and 0.5 nM for MCS0331 while the ULOQ was 25 nM and 50 nM, respectively (Table S2 and S3). The determined parameters of the analytical method validation for MPEP, MCS0455 and VU0409106 were detailed in[2].

MPEP Dissociation MS Binding Assays

$HmGlu_5$ membranes (20 μg/well) were incubated with 12 nM of MPEP for 1 h at 37°C, while shaking at 150 rpm and in a final assay volume of 300 μL/well, under dark conditions. Following the association phase, the dissociation of ligands was initiated with 10 μM VU0409106 at different time points (1 - 30 min), under dark, 500 nm or 380 nm conditions (50/50 ms off at 12V). Illumination of plates was performed as described in the main manuscript. The

assay was stopped and samples were analyzed as described in the main manuscript. Non-specific binding was determined in the presence of 10 μM VU0409106.

Animal behavioral studies

Behavioral studies

Mechanical pain threshold was evaluated with von Frey filaments (Bioseb, Vitrolles, France) using the simplified up-down method (SUDO method).[7] The forces applied were 0.02, 0.04, 0.07, 0.16, 0.4, 0.6, 1.0, and 1.4 g. Test began with the 0.16 g force filament. Baseline pain thresholds were assessed before implantations of the brain cannulas and after 1 week of recovery post-surgery. Optofluidic cannulas (Doric Lenses, Quebec, QC, Canada) were implanted unilaterally in the right amygdala by stereotaxic surgery as previously described (Bundel et al., 2016). Treatments delivered through cannulas were randomized. Mechanical threshold measurements were performed before and 8 days after induction of persistent inflammatory pain induced by intraplantar injection of 20 μl complete Freund's adjuvant (CFA; Sigma, France) in the left hind paw. For photopharmacology, we used a compact LED package combining two wavelengths (385 nm and 505 nm) coupled to a rotating optical fiber (fiber diameter: 200 μm, NA = 0.53). Each channel was controlled via the LED driver software (Doric Lenses, Quebec, QC, Canada). Mice were habituated to the optic fiber connection one week before the test. Mechanical allodynia was first tested 15 min after intra-amygdala injection of either alloswitch-1, MCS0331, MPEP or vehicle, in the absence of light stimulation. 385 nm or 505 nm wavelength light illumination (50 ms light pulses at 10 Hz frequency) was then applied, in 5 min intervals, starting with 385 nm at a light power of 8.0 mW (equalling 0.11 mW/mm^2), and 2.0 mW (equalling 0.029 mW/mm^2) for 505 nm wavelength, and the mechanical threshold for each cycle was assessed. After the behavioral study, mice were culled, brains were harvested and post-fixed for 2 hours in 4% PFA solution in PBS to check cannula locations. Animals were excluded from the study if cannulas were incorrectly implanted or removed by the mouse.

Data analysis

GraphPad prism version 8 (San Diego, CA) was used for all other curve fitting and statistical analysis. For photochemistry kinetic (*cis*-to-*trans* relaxation) experiments, half-life time ($t_{1/2}$) of the *cis*-alloswicth-1 and *cis*-MCS0331 were calculated by plotting absorbance readings at λ = 376 nm versus time and by fitting the obtained curve to an exponential decay function. ^{1}H-NMR spectra were analysed with Mnova version 8.1 software (Mestrelab).

For the direct determination of the functional agonist dissociation constants (K_A) from the receptor titration studies under different light conditions, glutamate and quisqualate concentration-response curves (in the presence of different amounts of transfected $mGlu_5$) were globally fitted to the operational model of agonism as previously described in [8-10].

For functional interaction studies between orthosteric agonists and allosteric modulators in the IP_1 assay, the following operational model of allosterism was applied.[11]

$$Y = Basal + \frac{(E_M - Basal) \cdot (\tau_A[A](K_B + \alpha\beta[B]) + \tau_B[B] \cdot K_A)^n}{([A]K_B + K_A K_B + K_A[B] + \alpha[A][B])^n + (\tau_A[A](K_B + \alpha\beta[B]) + \tau_B[B] \cdot K_A)^n}$$

(Equation 1)

Where Basal is the response in the absence of ligand, E_M is the maximum response of the system and *n* is the slope of the transducer function that links occupancy to response. [A] and [B] represent the concentrations of the orthosteric agonist (either glutamate or quisqualate) and allosteric ligand, respectively, and K_A and K_B denote their

respective equilibrium dissociation constants. τ_A and τ_B represent the relative efficacies of the orthosteric and allosteric ligands, respectively. α denotes the affinity cooperativity existing between the orthosteric agonist and allosteric modulator and β is the scaling factor, which defines the magnitude and the direction of the allosteric modulator effect on the agonist efficacy. For all datasets the τ_B was constrained to 0, since NAMs do not show allosteric agonism, the K_A was constrained to values derived from the receptor titration experiments for glutamate and quisqualate under different light conditions (glutamate(dark) pK_A = 4.58 ± 0.22; glutamate(500nm) pK_A = 4.60 ± 0.25; glutamate(380nm) pK_A = 4.51 ± 0.21; quisqualate(dark) pK_A = 7.26 ± 0.15; quisqualate(500nm) pK_A = 7.65 ± 0.28; quisqualate(380nm) pK_A = 7.28 ± 0.17), logα was constrained to 0, so the resulting logβ value was representative of the combined affinity and efficacy cooperativity estimates, that is log$\alpha\beta$, between the interaction of a modulator with an orthosteric agonist under different light conditions. The derived cooperativity values greater than 1 indicate positive cooperativity; values less than 1 but greater than 0 indicate negative cooperativity and values equal to unity denote neutral cooperativity.

In instances, where the application of equation 1 to interaction studies did not yield a reliable fit of the model or the model did not converge a scanning of parameters space based on reduction in global absolute sum-of-squares was performed [10, 12, 13]. Specifically, for the interaction of MCS0331 with glutamate (dark conditions) logα was constrained to 0, and in two separate analyses were performed, the logβ was constrained to values ranging from 0 to -3 or the $LogK_B$ was constrained to values ranging from –5 to –10, in either 0.05, 0.1 or 0.5 unit increments as Equation 1 was applied to the dataset under the aforementioned conditions until the global reduction in the sum of squares of the resulting fit approached an asymptotic value, thereby indicating that no additional improvement in the fit is possible by changing either the logβ or the $LogK_B$. From the application of this type of analysis, the reported $logK_B$ value was -7.50 for the interaction of MCS0331 with glutamate under dark conditions, (Supplementary Figure 2 and Table 1). This affinity estimate for the allosteric ligand was then used to fit the same interaction dataset according to Equation 1 to provide an estimate of the Logβ for the interaction, which is reported in Table 1.

For alloswitch-1,MCS0331 and MPEP MS binding studies, analysis was performed on Thermo Xcalibur 2.2 software (Qual Browser, Thermo Scientific) and GraphPad prism version 7.05 (San Diego, CA). Obtained peak areas were transformed to nmol of bound ligand using an appropriate calibration curve, which was based on the peak area of the analyte normalised by the corresponding IS compound versus the quantities (in nmol) of the analyte with weighted ($1/x^2$) least-squares linear regression.

For MS saturation binding studies, receptor expression (B_{max}) and equilibrium dissociation constants (K_D) for alloswitch-1 or MCS0331 were determined with the application of the following equation:

$$Y = \frac{B_{max}[A]}{[A] + K_A} + NS[A]$$

(Equation 2)

Where Y represents the bound ligand, B_{max} is the total receptor density, [A] is the ligand concentration, K_A is the equilibrium dissociation constant of the ligand, and NS represents the non-specific binding of the ligand. Estimates were reported in Table 2. Data were then represented as the logarithm of the concentration of bound ligand in Figure 4 and fitted to a standard logistic function to determine the functional potency (negative logarithm; pEC_{50}) and maximal responses (E_{max}).

For MS dissociation binding studies, dissociation rates (K_{off}) and half-lives of dissociation ($t_{1/2}$) for alloswitch-1, MCS0331 and MPEP were determined with the application of the following mono-exponential decay function:

$Y = \ln(2)/t_{1/2}$

(Equation 3)

For inhibition of [^{3}H]-MPEP equilibrium binding studies, data sets were fitted to a one-site inhibition binding model (equation 3). An extra sum-of-squares F-test was used to determine if there was any significant difference between the pK_I values of allosteric modulators in the presence or absence of saturating concentrations of orthosteric agonists, glutamate or quisqualate:

$$\frac{Y}{Y_{max}} = \frac{[A]}{A + \frac{K_D(1 + \frac{[B]}{K_I})}{(+ \frac{\alpha[B]}{K_I})}}$$

(Equation 4)

Where Y/Y_{max} represents the fractional specific binding, [A] is the concentration of the radioligand, [B] is the concentration of the allosteric modulator, the K_D is the radioligand equilibrium dissociation constant, K_B is the allosteric modulator equilibrium dissociation constant, and α is the binding cooperativity factor. An α value greater than 1 denotes positive cooperativity, while an α value less than 1 but greater than 0 denotes negative cooperativity, and an α value equal to 1 indicate neutral cooperativity.

All affinity, cooperativity and potency estimates are presented as logarithms except kinetic values and as expressed as the mean ± SEM.[14] Where appropriate, fitted parameters were compared by extra sum-of-squares F-test or statistical significance was determined with the use of one-way analysis of variance (ANOVA) with a Tukey's multiple comparisons post-hoc analysis using GraphPad Prism.[15] Significance was set at $P < 0.05$, unless otherwise stated. Behavioral studies were analyzed by Friedman test using GraphPad Prism and expressed as mean ± SEM.

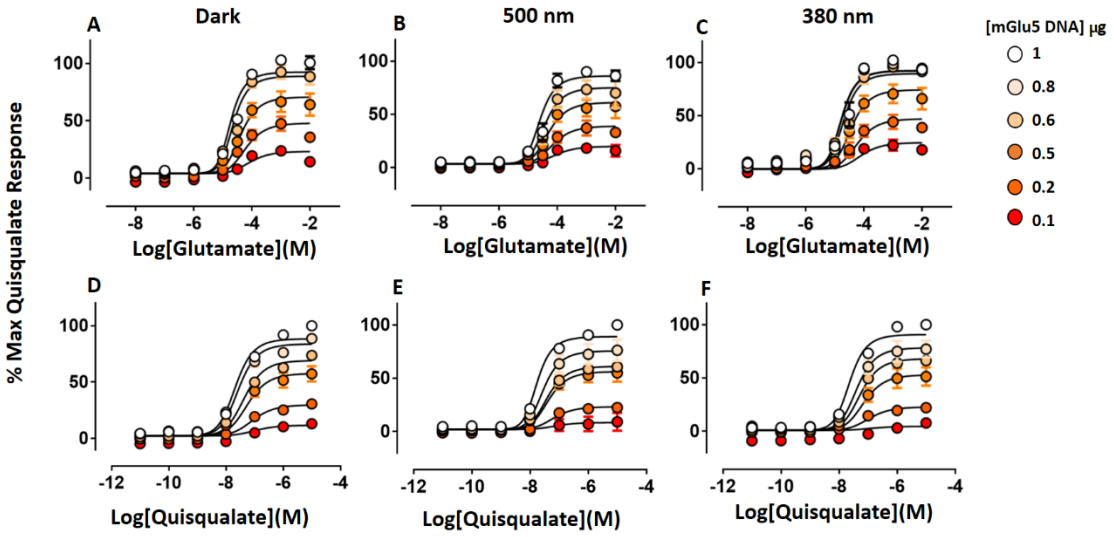

Fig. S1. Effect of receptor depletion on agonist-induced IP_1 accumulation under different light conditions. Effect of $hmGlu_5$ DNA concentration (0.1 - 1 mg per 10 million cells) on IP_1 accumulation stimulated by glutamate (A, B, C) or quisqualate (D, E, F) in HEK cells transiently transfected with $hmGlu_5$ and the excitatory amino acid transporter (EAAT) under different light conditions. Data are expressed as a % of maximal quisqualate response as determined by a fixed concentration of quisqualate (10 µM) acting on cells that were transfected with 1 mg of $hmGlu_5$ DNA per 10 million cells and represent the mean ± SEM of at least three independent experiments performed in duplicate.

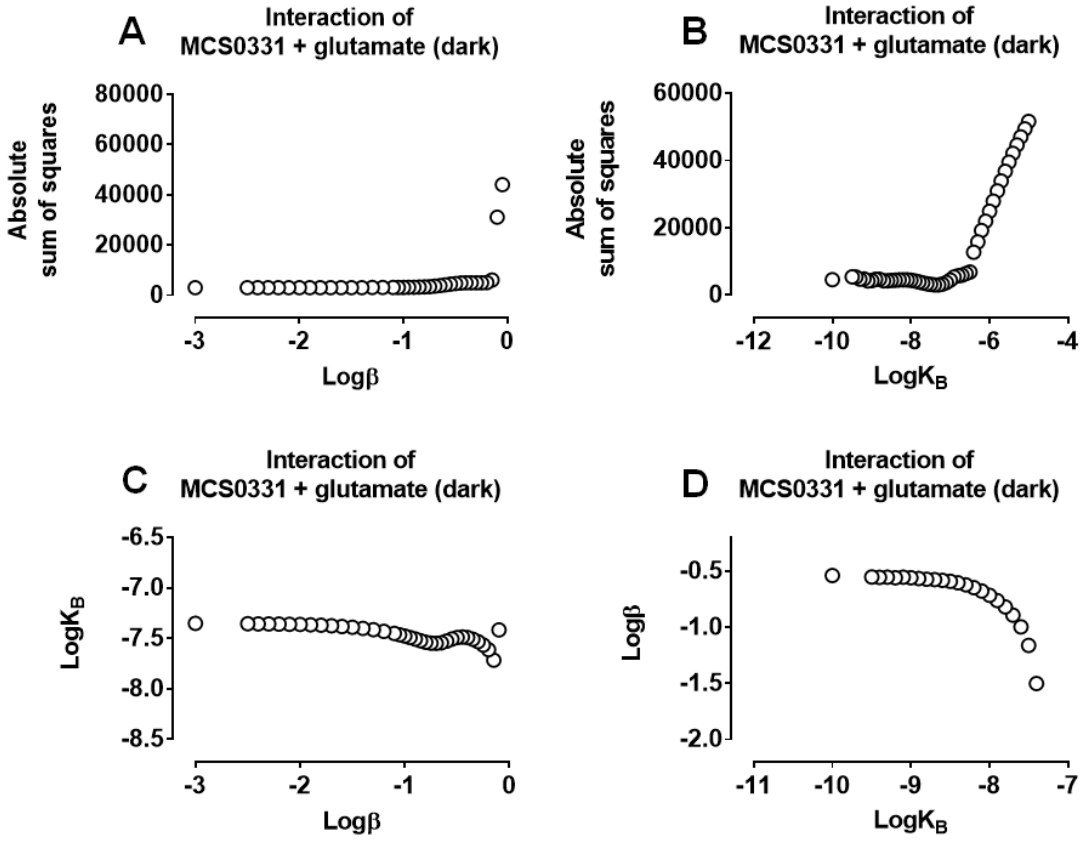

Fig. S2. Absolute sum-of-squares analyses performed for the interaction between MCS0331 and glutamate under dark condition in an IP_1 accumulation assay. Absolute sum-of-squares analyses were performed to determine an estimate for the negative cooperativity (logβ) or allosteric ligand affinity ($LogK_B$) for the interaction between MCS0331 and glutamate (dark). Specifically, equation 1 was consecutively applied while the logβ was constrained to values ranging from '0 to '-3, in either 0.05, 0.1 or 0.5 unit increments (**A**) or when the $LogK_B$ was constrained to values ranging from –5 to –10, in either 0.05, 0.1 or 0.5 unit increments (**B**). The reported $logK_B$ value (Table 1) represents the value obtained when the minimum mean squared error for each curve fit began to reach an asymptotic value (as indicated in the above Figure). These values were then used as constants to fit IP_1 accumulation interaction datasets according to Equation 1 (Table 1). Panel **C** and **D** illustrate the resulting $LogK_B$ or Logβ values that are generated when Logβ or $LogK_B$ values are, respectively, constrained to fixed values during the absolute sum-of-squares analysis.

.

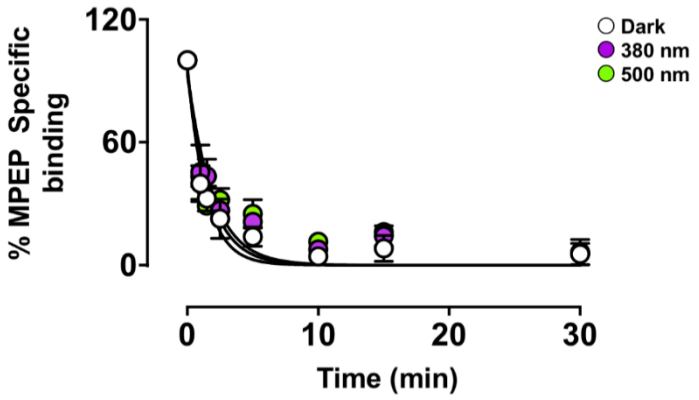

Fig. S3. MPEP MS dissociation experiments performed under different light conditions. 12 nM of MPEP was incubated with $hmGlu_5$ expressing membranes for 1h at 37ºC under dark conditions, and dissociation half-lives (Table 3) were then determined by the addition of a saturating concentration of the competitive NAM, VU409106, at different time points under dark, 500 nm and 380 nm light conditions. Data are expressed as a percentage of specific binding and represent the mean ± SEM of three independent experiments performed in duplicate.

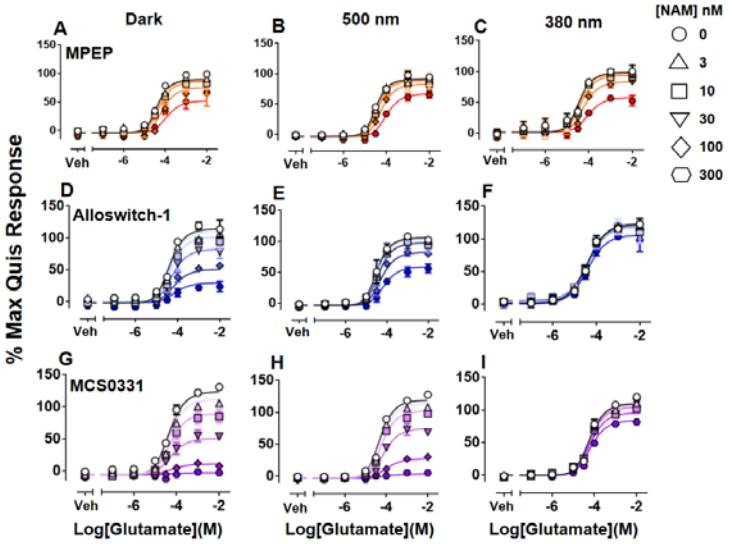

Fig. S4. (Non)Photoswitchable NAMs have comparable NAM activity at the mouse $mGlu_5$ under different light conditions. Effect of light on the ability of the $mGlu_5$ NAMs, MPEP (A, B, C), alloswitch-1 (D, E, F), or MCS0331 (G, H, I) to negatively modulate glutamate-stimulated IP_1 accumulation in HEK cells transiently transfected with the mouse $mGlu_5$. Data are expressed as a % of maximal quisqualate response, as determined by a fixed concentration of quisqualate (quis; 10 μM), and represent the mean ± SEM of at least three independent experiments performed in duplicate. Fitted curves are from global analysis of datasets according to Equation 1 (in Methods) with parameter estimates shown in supplementary table 4.

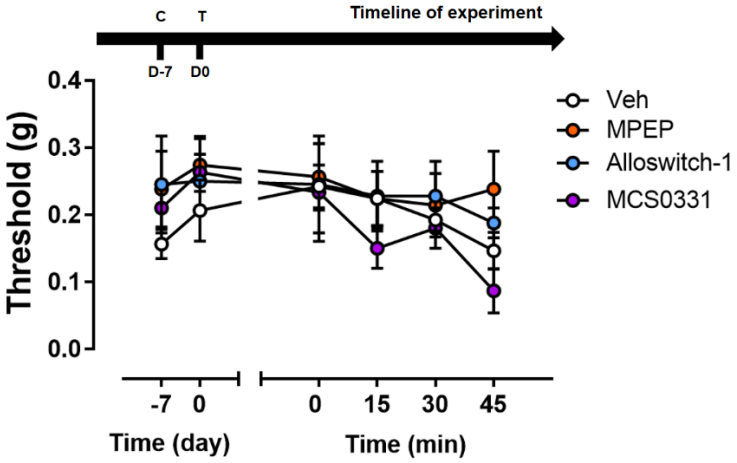

Fig. S5. Intra-amygdala injection of (non)photoswitchable $mGlu_5$ NAMs do not affect the mechanical pain threshold of naïve mice. The mechanical pain threshold of naïve animals was evaluated by stimulating the hind paw of mice with von Frey filaments, following intra-amygdala injection of either vehicle (n = 5), MPEP (1 mM; n = 5), alloswitch-1 (300 nM; n = 4) or MCS0331 (300 nM; n = 3). Data were expressed as mean ± SEM. Timeline of experiment; "C" refers to the day of intra-amygdala cannulation, "T" refers to test day where mice received either vehicle or NAM treatment.

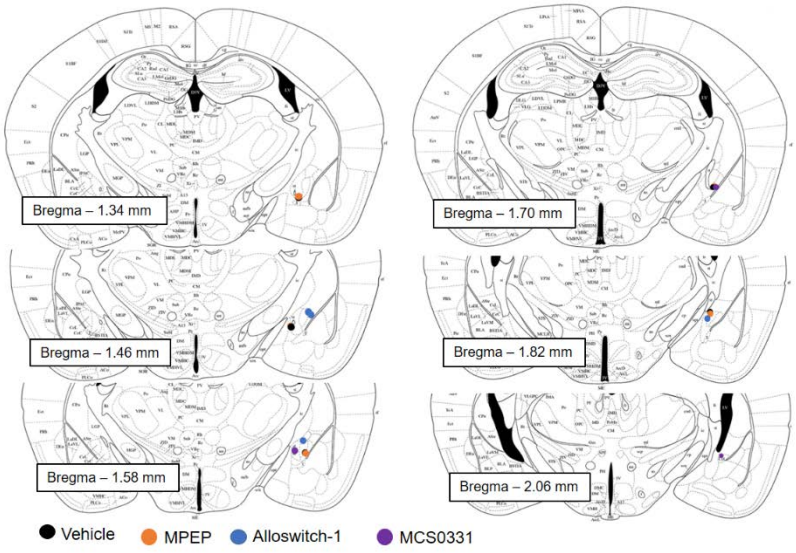

Fig. S6. Neuroanatomical validation of injection sites for $mGlu_5$ NAM or vehicle treated rats.

Table S1. Operational model parameters for agonist-induced IP_1 accumulation under different light conditions in cells transfected with different amounts of $hmGlu_5$ DNA. Data represent the mean ± SEM of at least three independent experiments performed in duplicate.

	[a]pK_A			[b]Log τ (τ)		
	Dark light	**500 nm**	**380 nm**	**Dark light**	**500 nm**	**380 nm**
Quisqualate	7.26 ± 0.15	7.65 ± 0.28	7.28 ± 0.17	0.19 ± 0.04 (1.55)	0.07 ± 0.04 (1.17)	0.16 ± 0.04 (1.44)
Glutamate	4.58 ± 0.22	4.60 ± 0.25	4.51 ± 0.21	0.30 ± 0.10 (2.0)	0.15 ± 0.07 (1.41)	0.37 ± 0.11 (0.37)

[a]Negative logarithm of the equilibrium dissociation constant of the indicated agonist under different light conditions.

[b]Negative logarithm of the operational efficacy parameter for each dataset (antilog shown in parentheses).

Datasets were analysed according to a operational model of agonism.

Table S2. Within- and between-run accuracy and precision of analytical method to determine alloswitch-1 signal (n = 3 r, 5 replicates per run). Quality control (QC) samples with final concentrations of 0.125 nM (Lower limit of quantification; LLOQ), 0.35 nM (Lower; L), 10 nM (Medium; M), 20 nM (Higher; H) and 25 nM (Upper limit of quantification; ULOQ) were prepared in acetonitrile: 10 mM ammonium bicarbonate, pH 7 (3:1). The criteria for the data included accuracy (relative error, RE) and a precision (relative standard deviation, RSD) within ± 20 % (except ± 25 % for the LLOQ and ULOQ).

	Within-run		**Between-run**	
Spiked concentration (nM)	**Accuracy (RE, %)**	**Precision (RSD, %)**	**Accuracy (RE, %)**	**Precision (RSD, %)**
0.125	10.6	13.0	6.8	10.8
0.35	8.4	7.9	10.7	9.2
10	4.9	8.4	1.4	5.6
20	8.3	6.6	1.4	6.6
25	- 3.9	7.0	- 0.4	5.1

Table S3. Within- and between-run accuracy and precision of analytical method to determine MCS0331 signal (n = 3 r, 5 replicates per run). Quality control (QC) samples with final concentrations of 0.5 nM (Lower limit of quantification; LLOQ), 1.25 nM (Lower; L), 20 nM (Medium; M), 37.5 nM (Higher; H) and 50 nM (Upper limit of quantification; ULOQ) were prepared in acetonitrile: 10 mM ammonium bicarbonate, pH 7 (3:1). The criteria for the data included accuracy (relative error, RE) and a precision (relative standard deviation, RSD) within ± 20 % (except ± 25 % for the LLOQ and ULOQ).

	Within-run		**Between-run**	
Spiked concentration (nM)	**Accuracy (RE, %)**	**Precision (RSD, %)**	**Accuracy (RE, %)**	**Precision (RSD, %)**
0.5	11.9	11.7	5.1	11.0
1.25	17.5	10.4	10.3	10.5
20	17.1	11.5	7.0	13.7
37.5	- 13.0	9.1	- 0.6	10.6
50	- 11.7	8.7	- 3.9	10.1

Table S4. Summary of MPEP dissociation kinetic parameter estimates under different light conditions as determined by MS binding assays.

	Dark		500 nm		380 nm	
	[a]k_{off} (min^{-1})	[b]$t_{1/2}$ (min)	[a]k_{off} (min^{-1})	[b]$t_{1/2}$ (min)	[a]k_{off} (min^{-1})	[b]$t_{1/2}$ (min)
MPEP	1.06 ± 0.24	0.74 ± 0.21	0.55 ± 0.05	1.27 ± 0.12	0.62 ± 0.14	1.25 ± 0.28

[a]Dissociation rate of the indicated NAM.

[b]$t_{1/2}$ is the half-life of dissociation.

No significative difference in the dissociation rate was determined by one-way ANOVA, which is performed on the logarithm of the k_{off} values as the values are log normally distributed.

Table S5. Operational model of allosterism parameters for interactions at mouse $mGlu_5$.

allosteric ligand	Dark			500 nm			380 nm		
	[a]pK_A	[b]pK_B	[c]Log αβ (αβ)	[a]pK_A	[b]pK_B	[c]Log αβ (αβ)	[a]pK_A	[b]pK_B	[c]Log αβ (αβ)
MPEP	4.02 ± 0.17	6.91 ± 0.20	= -1[$] (0.10)	3.95 ± 0.11	6.95 ± 0.12	-0.96 ± 0.22 (0.11)	4.15 ± 0.17	6.81 ± 0.17	-1.18 ± 0.30 (0.07)
alloswitch-1	4.37 ± 0.11	7.32 ± 0.13	-0.71 ± 0.13 (0.19)	4.24 ± 0.09	6.89 ± 0.15	-0.86 ± 0.27 (0.14)	n.d.	n.d.	n.d.
MCS0331	4.58 ± 0.12	7.42 ± 0.15	-1.38 ± 0.57	4.29 ± 0.07	7.44 ± 0.08	-1.22 ± 0.18	n.d.	n.d.	n.d.

[a]Negative logarithm of the equilibrium dissociation constant for glutamate.

[b]Negative logarithm of the allosteric modulator equilibrium dissociation constant.

[c]Logarithm of the efficacy scaling factor (antilog values shown in parentheses) for the effect of the indicated NAM on glutamate responses under different light conditions; when the logarithm of the affinity cooperativity between the agonist and the NAM is equal to zero ($\log\alpha = 0$), it is equivalent to the combined functional cooperativity between ligands ($\log\alpha\beta$). Combined cooperativity values with a corresponding $ were derived from applying an absolute sum of squares analysis.

Estimated parameters represent the mean ± SEM of at least three experiments performed in duplicate. Functional IP_1 accumulation responses were analysed according to Equation 1.

SI References

1. Gomeza, J., Mary, S., Brabet, I., Parmentier, M. L., Restituito, S., Bockaert, J., and Pin, J. P. (1996) Coupling of metabotropic glutamate receptors 2 and 4 to G alpha 15, G alpha 16, and chimeric G alpha q/i proteins: characterization of new antagonists, *Molecular pharmacology 50*, 923-930. PMID: 8863838.
2. Ricart-Ortega, M., Berizzi, A. E., Catena, J., Malhaire, F., Muñoz, L., Serra, C., Pinc, J., Lebon, G., Goudet, C., and Llebaria, A. (2020) Development and validation of a Mass Spectrometry binding assay for mGlu5 receptor, *Analytical and bioanalytical chemistry 412*, 5525-5535. DOI: 10.1007/s00216-020-02772-9.
3. Gomez-Santacana, X., Pittolo, S., Rovira, X., Lopez, M., Zussy, C., Dalton, J. A., Faucherre, A., Jopling, C., Pin, J. P., Ciruela, F., Goudet, C., Giraldo, J., Gorostiza, P., and Llebaria, A. (2017) Illuminating Phenylazopyridines To Photoswitch Metabotropic Glutamate Receptors: From the Flask to the Animals, *ACS central science 3*, 81-91. DOI: 10.1021/acscentsci.6b00353.
4. Sun, X., Shan, G., Sun, Y., and Rao, Y. (2013) Regio- and Chemoselective C-H Chlorination/Bromination of Electron-Deficient Arenes by Weak Coordination and Study of Relative Directing-Group Abilities, *Angewandte Chemie International Edition 52*, 4440-4444. DOI: 10.1002/anie.201300176.
5. Llebaria, A., Gorostiza Langa, P., GÓMEZ SANTACANA, Pittolo, S., Giraldo Arjonilla, J., Rovira Algans, X., Goudet, C., and Pin, J. (2013) Glutamate receptor photomodulators, *WO2015044358A2*.
6. Administration, U. D. o. H. a. H. S. F. a. D. (2018) Guidance for industry: bioanalytical method validation
7. Bonin, R. P., Bories, C., and De Koninck, Y. (2014) A simplified up-down method (SUDO) for measuring mechanical nociception in rodents using von Frey filaments, *Molecular pain 10*, 26. DOI: 10.1186/1744-8069-10-26.
8. Black, J. W., and Leff, P. (1983) Operational models of pharmacological agonism, *Proceedings of the Royal Society of London. Series B, Biological sciences 220*, 141-162. DOI: 10.1098/rspb.1983.0093.
9. Berizzi, A. E., Gentry, P. R., Rueda, P., Den Hoedt, S., Sexton, P. M., Langmead, C. J., and Christopoulos, A. (2016) Molecular Mechanisms of Action of M5 Muscarinic Acetylcholine Receptor Allosteric Modulators, *Molecular pharmacology 90*, 427-436. DOI: 10.1124/mol.116.104182.
10. Berizzi, A. E., Bender, A. M., Lindsley, C. W., Conn, P. J., Sexton, P. M., Langmead, C. J., and Christopoulos, A. (2018) Structure-Activity Relationships of Pan-Galphaq/11 Coupled Muscarinic Acetylcholine Receptor Positive Allosteric Modulators, *ACS chemical neuroscience 9*, 1818-1828. DOI: 10.1021/acschemneuro.8b00136.
11. Leach, K., Sexton, P. M., and Christopoulos, A. (2007) Allosteric GPCR modulators: taking advantage of permissive receptor pharmacology, *Trends in pharmacological sciences 28*, 382-389. DOI: 10.1016/j.tips.2007.06.004.
12. Dror, R. O., Green, H. F., Valant, C., Borhani, D. W., Valcourt, J. R., Pan, A. C., Arlow, D. H., Canals, M., Lane, J. R., Rahmani, R., Baell, J. B., Sexton, P. M., Christopoulos, A., and Shaw, D. E. (2013) Structural basis for modulation of a G-protein-coupled receptor by allosteric drugs, *Nature 503*, 295-299. DOI: 10.1038/nature12595.
13. Ehlert, F. J. (1985) The relationship between muscarinic receptor occupancy and adenylate cyclase inhibition in the rabbit myocardium, *Molecular pharmacology 28*, 410-421.
14. Christopoulos, A. (1998) Assessing the distribution of parameters in models of ligand-receptor interaction: to log or not to log, *Trends in pharmacological sciences 19*, 351-357. DOI: 10.1016/s0165-6147(98)01240-1.
15. Motulsky, H., and Christopoulos, A. (2004) Fitting models to biological data using linear and nonlinear regression: a practical guide to curve fitting, *Oxford University Press, Oxford*.